Synthesis and Thio-Functionalization of Metal Organic Frameworks of Isonicotinate Ligands andTheir application for fluorescein removal from aqueous solution

ABSTRACT

Mechanochemical syntheses of four (4) know metal organic frameworks (MOFs) were obtained by grinding stoichiometric amounts of metal salts [Zn(II) and Cu(II)] and corresponding carboxylate ligands [Fumaric and Isonicotinic acids] in a mortar with a pestle. Also, Solvent-based syntheses of MOFs were carried out with the reaction of metal salts and each carboxylate ligand by mixing in the presence of solvents. The compounds were characterized by the comparison of melting point, elemental analysis, FT-IR spectroscopy and XRPD results with those of the free ligands and literature. The analytical and spectroscopic data of the compounds prepared via the two different methods gave the expected product.

The presence of coordinatively unsaturated metal centers in the synthesized MOFs provides an accessible way to selectively functionalize them through coordination bonds. In this work, thiol-functionalization of MOFs were described by choosing six well known MOFs in which three (3) are Zn-based while the other three (3) are Cu-based MOF, by a facile coordination based postsynthetic strategy. The obtained thiol-functionalized MOFs were characterized by powder X-ray diffraction, CHN and infrared spectroscopy. The analytical and spectroscopic data of the unmodified and modified compound were different.

A series of $[Cu(Ina)_2]$ samples stoichiometrically decorated with thiol groups has been prepared through coordination bonding of coordinatively unsaturated metal centers with –SH group in thioglycolic acid. $[Cu(Ina)_2].H_2O$ and $[Cu(Ina)_2]$-TH were investigated for the adsorptive removal of fluorescein from aqueous solution. The parameters that affect the dye sorption such as contact time, solution pH, initial fluorescein concentration and temperature, have been investigated and optimized conditions determined at PH of 7.8. Dubinin–RadushkevichEquilibrium isotherm studies were used to evaluate the maximum sorption capacity of MOFs and experimental results showed that the removal efficiency decreases in the order of

[$Cu(Ina)_2$]-TH > [$Cu(Ina)_2$].H_2O both in adsorption rate and adsorption capacity. The Langmuir, Freundlich, Temkin and DubininRadushkevich models have been applied and the data correlate well with DubininRadushkevich model. The adsorption mechanism may be explained with a simple electrostatic interaction and π- π interaction. Finally, it can be suggested that modification of MOFs can be use to improve their adsorption capacity and rate, making them a better adsorbent to remove emerging dyes contaminants from waste water.

Key word:Mechanochemical syntheses, metal organic frameworks, postsynthetic, thermogravimetris, Isonicotinic, FT-IR, Aqueous Solution, Removal of Dye

INTRODUCTION

During the past century particularly around 1960, extensive work was done on crystalline extended structures (Porous materials) in which metal ions are joined by organic linkers containing Lewis base–binding atoms such as nitriles and bipyridines [1]. These were recognized as coordination polymers and were first reported by Tomic [2]. The metal ions which act as the center connector are usually chosen from Cu, Zn, Mn, and Co. The connectors-linkers building blocks form continuous porous network structures that can be classified by porous structure as dots (0 D cavity), channels (1D space), layers (2D space), and intersecting channels (3D space). Based on the porous structure, coordination polymer can be applied in separation, storage, and heterogeneous catalysis. However, a more general term Metal-Organic Frameworks was introduced, and has attracted great attention.

A typical structure of MOF

The superior characteristics and properties of porous MOF [6] when compared to traditional porous carbon materials and inorganic zeolites is the drive behind its rapid development in science world. These include the possibility to design the structures and sizes of their pore by carefully choosing metal ions and organic ligands because of the wide variety of coordination geometries offered by transition and lanthanide metal ions; and the varsity of structures and reactive functionalities that can be incorporated into organic linkers via organic synthesis [7].

Also, unlike zeolites, which form channels ranging from 3-12 Å in diameter, MOFs allow for much greater internal void space and larger channels (up to 20- 30Å) in which guests can resides.[8, 9]

1.2POROUS MATERIAL

Porous solids are group of materials that have pores or channels that run through their structures that are permeable to the diffusion of guest molecules such as air or water. Most porous solids have porosities from 0.2 to 0.95, defined by the fraction of void accessible to guests to the total volume occupied by the solid material itself [10]. Porous solids can be generally divided into two broad classes, amorphous (disordered) solids and ordered (crystalline) solids.

1.2 METAL ORGANIC FRAMEWORKS

Metal-Organic Frameworks are crystallinecompounds consisting of metalionsorclusterscoordinated to rigid organic moleculesto form one-, two-, or three-dimensional structures that can be porous[36]. Metal-Organic Frameworks (MOFs) are a class of hybrid materials which are constructed by metal nodes and organic linkers forming highly porous structures. The careful selection of MOF building blocks such that their properties are retained by the framework can yield unique materials with a host of physical and optical characteristics and applications. The nature of the linkers often leads to voids present in the structure; these are usually occupied by guest molecules, which interact with the framework and need to be removed or exchanged for the MOF to be activated.

One of the most important properties of MOFs is their high structure porosity exhibiting high pore volume (up to 90 % of the crystal volume) and high specific surface area (up to several 2 -1 [36-40] thousand m g). The wide-open MOF structures with well-defined pores with internal diameters of up to 48 Å provide extra-large free space for loading with guest molecules making MOFs promising host materials for applications in energy (H /CH gas) storage molecule adsorption and separation, nano particle in-pore assembly, catalysis. MOFs are also of great importance in their use as drug delivery agent due to their properties; exceptionally high surface area and large pore sizes.

1.5 MOFs STRUCTURE

A metal-organic framework (MOF) is composed of two major components: a metal ion or cluster of metal ions and an organic molecule called a linker. The organic units are typically mono-, di-, tri-, or tetravalentligands.[53] The choice of metal and linker has significant effects on the structure and properties of the MOF, for example, the metal's coordinationpreference influences the size and shape of pores by dictating how many ligands can bind to the metal and in which

[54] orientation. the metal nodes (metal ions or metal-including clusters) serve as connecting points and the organic ligands serve as bridging molecules to coordinately connect metal nodes forming a three-dimensional framework.

Although varying valency of the transition metals may seem to expand the number of potential structures to be produced with diminishing ability to predict structural architecture, this problem can be solved by carefully changing reaction conditions to favour a particular coordination number and geometry.[53, 54]Recently the generation of frameworks with new and unusual network topologies has seen the emergence of lanthanides as metal centres. Lanthanide metal ions commonly have the oxidation state 3^+ and possess large ionic radii. Therefore binding is non-directional and electrostatic with steric factors often directing the coordination geometries of resulting frameworks.

1.16 AIM AND OBJECTIVES

The primary aim of this research project is to functionalize metal-organic framework (MOFs) initially synthesized and also to apply both the functionalized and unfunctionalized MOFs for environmental remediation.

The objectives of this research work are to:

i. Use room temperature solvent based and mechanochemical solvent free synthetic methods to prepare some of the MOFs that had been synthesized previously by hydrothermal/solvothermal methods thereby allowing large scale production of MOFs in industries.

ii. To characrerize the synthesized MOFs using Melting point, Elemental Analysis, IR spectroscopy and XRPD.

iii. Use the functionalized and unfunctionalized MOFs for removal of dyes from aqueous solution.

1.17 JUSTIFICATION

A principal challenge of modern chemistry is to develop new energy, solvent and atom efficient approaches to chemical synthesis in order to aid the chemical industry in managing the global problem of pollution, growing energy demand and a shortage of raw materials.

Environmental problem associated with disposal of waste in most chemical reactions have led chemists to consider alternative environmental friendly preparative methods. For instance, one of the major targets of green chemistry is to limit the excessive use of solvents or even better to carry out the synthetic reactions in absence of solvents.

MOFs are a new class of crystalline materials which are currently of great interest for sorption, separation, drug delivery and catalysis. MOFs have been mainly synthesized at relatively high temperature by hydrothermal or solvothermal methods using conventional heating. However, these methods suffer from several drawbacks such as high temperature, long reaction times, excess organic solvents, lower product yields and harsh refluxing conditions. Solvothermal conditions are unsuitable for thermally- sensitive starting materials. Due to the aforementioned drawback of the solvothermal and hydrothermal syntheses, this research was focused on the use of room temperature solution based synthesis which does not require heat for the synthesis of MOFs.

2.4. THIOL-FUNCTIONALIZATION OF THE SYNTHESIZED MOFs

To prepare the thiol-functionalized MOFs samples, the method used by Ling-Guang *et al.*[124]was modified. The schematic illustration of the thiol-functionalization of MOFs is shown below

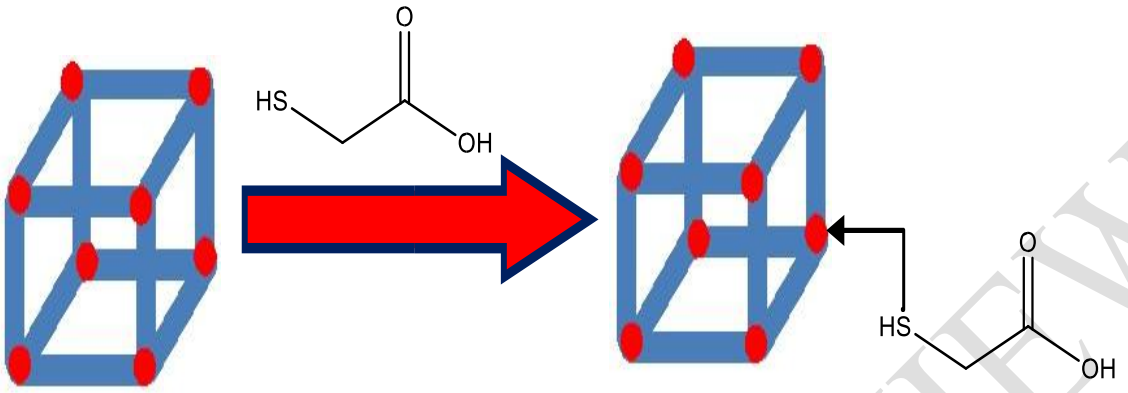

Fig.1. Schematic illustration of the thiol-functionalization of MOFs through coordination bonding between one thiol group of Thioglycolic Acid and coordinatively unsaturated metal centers (UMCs) in MOFs.

2.4.1. THIOLATION OF $[Cu(INA)_2]$

$[Cu(INA)_2]$ (0.620 g, 2 mmol) was dehydrated at 150 ◦C for 12 h and then suspended in 10 mL of anhydrous ethanol. Thioglycolic (0.091 ml, 1 mmol) was added to the suspension and the mixture solution was refluxed magnetically for 12 h at 80 ^{o}C. Cream flake crystal was obtained which was recovered by filtration, washed with ethanol (15 mL × 5) and then dried overnight at room temperature in vacuum. The relative content of S in the functionalized sample was determined by elemental analysis. This was done in batches to produce the quantity needed for the removal of dyes.

2.4.2. THIOLATION OF $[Zn(INA)_2$

$[Zn(INA)_2]$ (0.619 g, 2 mmol) was dehydrated at 100 ◦C for 12 h and then suspended in 10 mL of anhydrous toluene. Thioglycolic (0.091 ml, 1 mmol) was added to the suspension and the mixture solution was stirred magnetically for 12 h at 150 ^{o}C. Light yellow flake crystal was obtained which was recovered by filtration, washed with ethanol (15 mL × 5) and then dried overnight at room temperature in vacuum. The relative content of S in the functionalized sample was determined by elemental analysis.

2.4.3. THIOLATION OF [Zn(fum)(H_2O)$_2$]

[Zn(fum)(H_2O)$_2$] (0.431 g, 2 mmol) was dehydrated at 150 ◦C for 12 h and then suspended in 10 mL of anhydrous toluene. Thioglycolic (0.091 ml, 1 mmol) was added to the suspension and the mixture solution was refluxed magnetically for 12 h at 150 ^{o}C. Yellow flake crystal was obtained which was recovered by filtration, washed with ethanol (15 mL × 5) and then dried overnight at room temperature in vacuum. The relative content of S in the functionalized sample was determined by elemental analysis.

2.4.4. THIOLATION OF [Zn_2(fum)$_2$(bpy)]

[Zn_2(fum)$_2$(bpy)] (1.030 g, 2 mmol) was dehydrated at 150 ◦C for 12 h and then suspended in 10 mL of anhydrous toluene. Thioglycolic (0.091 ml, 1 mmol) was added to the suspension and the mixture solution was stirred magnetically for 12 h at 150 ^{o}C. Yellow flake crystal was obtained which was recovered by filtration, washed with ethanol (15 mL × 5) and then dried overnight at room temperature in vacuum. The relative content of S in the functionalized sample was determined by elemental analysis.

2.4.5. THIOLATION OF [Zn_4O(bdc)$_3$]

[Zn_4O(bdc)$_3$] (2.932 g, 2 mmol) was dehydrated at 150 ◦C for 12 h and then suspended in 10 mL of anhydrous toluene. Thioglycolic (0.091 ml, 1 mmol) was added to the suspension and the mixture solution was refluxed magnetically for 12 h at 150 ^{o}C. Yellow flake crystal was obtained which was recovered by filtration, washed with ethanol (15 mL × 5) and then dried overnight at room temperature in vacuum. The relative content of S in the functionalized sample was determined by elemental analysis.

2.4.6. THIOLATION OF [Cu_3(BTC)$_2$]

[Cu_3(BTC)$_2$] (2.932 g, 2 mmol) was dehydrated at 150 ◦C for 12 h and then suspended in 10 mL of anhydrous toluene. Thioglycolic (0.091 ml, 1 mmol) was added to the suspension and the mixture solution was stirred magnetically for 12 h at 150 ^{o}C. Black flake crystal was obtained which was recovered by filtration, washed with ethanol (15 mL × 5) and then dried overnight at

room temperature in vacuum. The relative content of S in the functionalized sample was determined by elemental analysis.

2.5. PHYSICAL AND INSTRUMENTAL CHARACTERIZATION METHODS

2.5.1 Melting Point – The melting point of the synthesized metal-organic frameworks were determined using a Gallen-Kamp melting point apparatus at the department of Chemistry, University of Ilorin.

2.5.2 Element Analysis – The elemental analyses were performed on a Perkin-Elmer CHN Analyzer 2400 series II at Medac Ltd, Brunnel Science Centre, Egham, United Kingdom.

2.5.3 Infrared Spectra – The infrared analyses were done using the SHIMADZU scientific model FTIR 8400s Spectrophometer at Redeemer's University, Ogun State. IR spectra on the range of 4,000-400 cm^1were obtained from samples in the form of KBr pellets.

2.5.4 X-ray Powder Diffraction Analysis –XRPD analyses were carried out at the Chemistry Department, University of Cape town, South Africa. Powder XRD analysis were measured on a Bruker D8 Advance X-ray diffractometer operating in a Da Vinci geometry equipped with Lynxeye detector using a CuKα-radiation(λ= 1.5406 Å).X-rays were generated by an accelerating voltage of 30kV and a current flow of 40mA. A receiving slit of 0.6mm and a primary secondary slits of 2.5mm were used. Samples were placed on a zero background sample holder and scanned over a range of 4^o to $40^o$with a step size of $0.01^o s^{-1}$.

2.6. DYES ADSORPTION PROCEDURE.

Batch equilibrium technique was used to study adsorption of fluorescein on $[Cu(Ina)_2].H_2O$ and $[Cu(Ina)_2]$-TH. An aqueous stock solution of fluorescein (100 ppm) was prepared by dissolving 100mg of fluorescein in 1L of deionized water. Aqueous dye solutions with different concentrations of the fluorescein (3 - 21 ppm) were prepared by successive dilution of the stock solution with deionized water. The concentration of fluorescein was determined using the absorbance (at λ_{MAX} = 490nm) of the solutions after getting the UV spectra of the solution with a

spectrophotometer (SHIMADZU UV-1650pc UV-VIS spectrophotometer). The calibration curve was obtained from the spectra of the standard solutions (3 - 21 ppm) at a pH of 7.8.

Before adsorption, the Adsorbents ($[Cu(Ina)_2].H_2O$ and $[Cu(Ina)_2]$-TH) were activated by drying overnight under vacuum at $150^{O}C$ and kept in a desiccator. An exact amount of the adsorbents (2mg) were put into the aqueous solutions (50mL) with the fixed dye concentration from 3 ppm to 21 ppm. The aqueous fluorescein solutions containing adsorbents (MOFs) were mixed well with an incubator shaker at 165 rpm and were maintained for a fixed time (10 min to 6 h) at 32 $\pm$ 2 ^{O}C. After adsorption for a pre-determined time, the solutions were separated from adsorbent (MOFs) using syringe filter, and the dyes concentration was calculated with the absorbance that would be obtained from the UV spectrophotometer.

2.7. ADSORPTION ISOTHERMS

Adsorption Isotherms show the relationship between the amount of dye adsorbed and the concentration of the dye at constant temperature.

2.7.1. LANGMUIR ISOTHERM

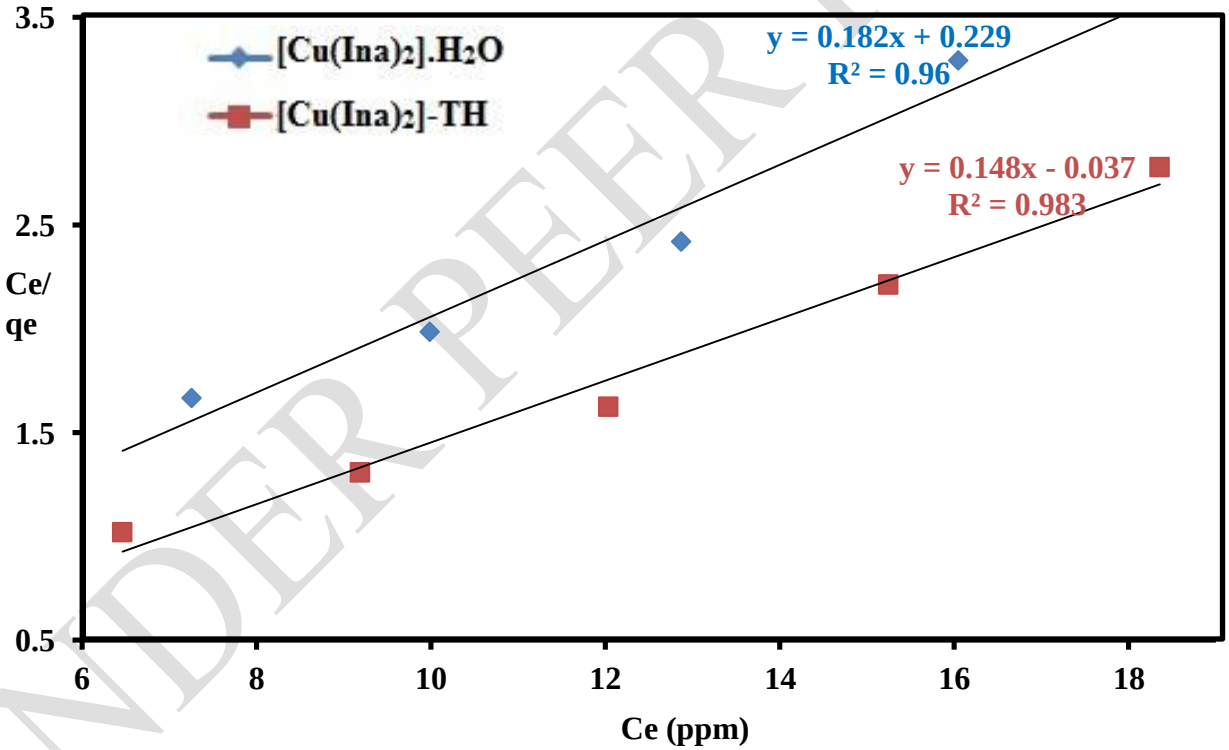

Fig 2: Langmuir isotherm plot of the Fluorescein adsorption.

2.7.2. FREUNDLICH ISOTHERM

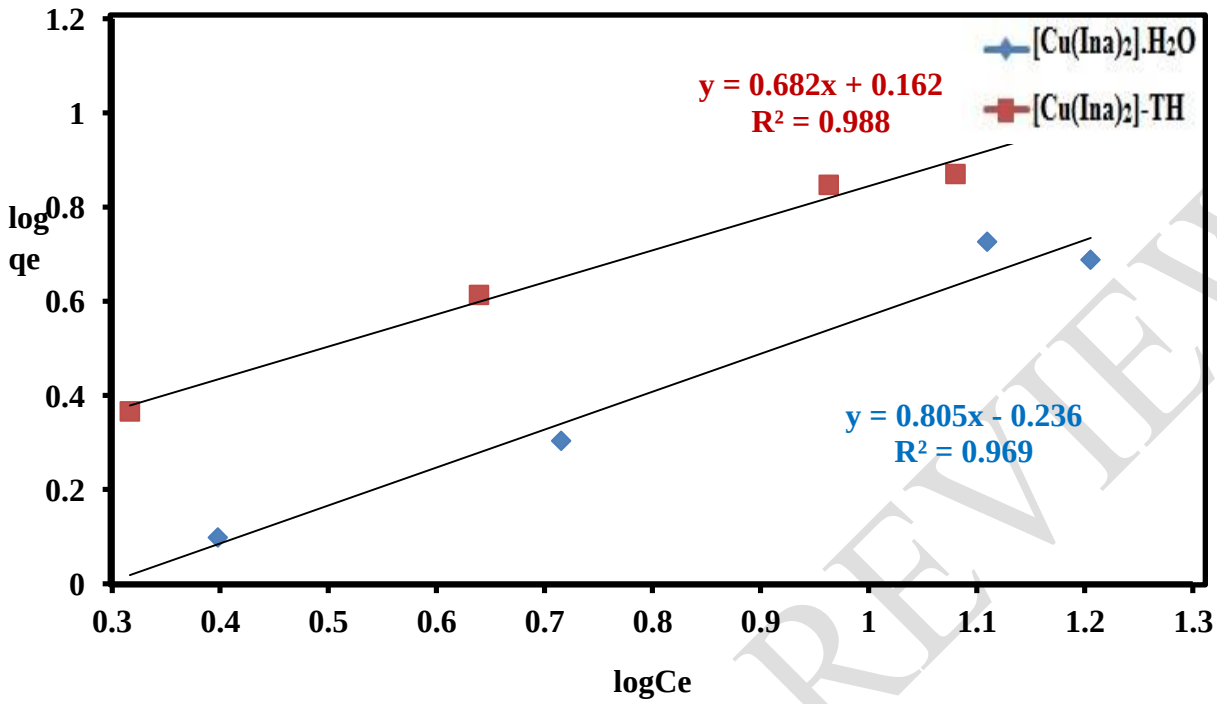

Fig 3: Freundlich isotherm plot of the Fluorescein adsorption

2.7.3 **TEMKIN ISOTHERM**

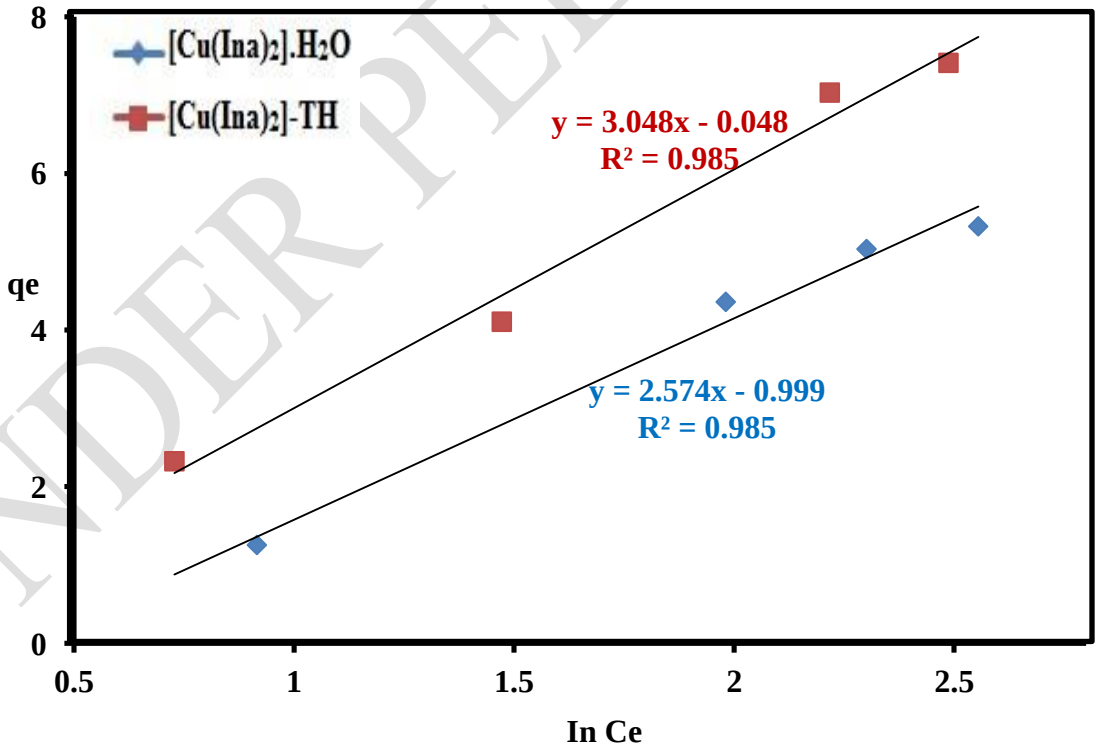

Fig 4: Temkin isotherm plot of the Fluorescein adsorption

2.7.DUBININ–RADUSHKEVICH ISOTHERM

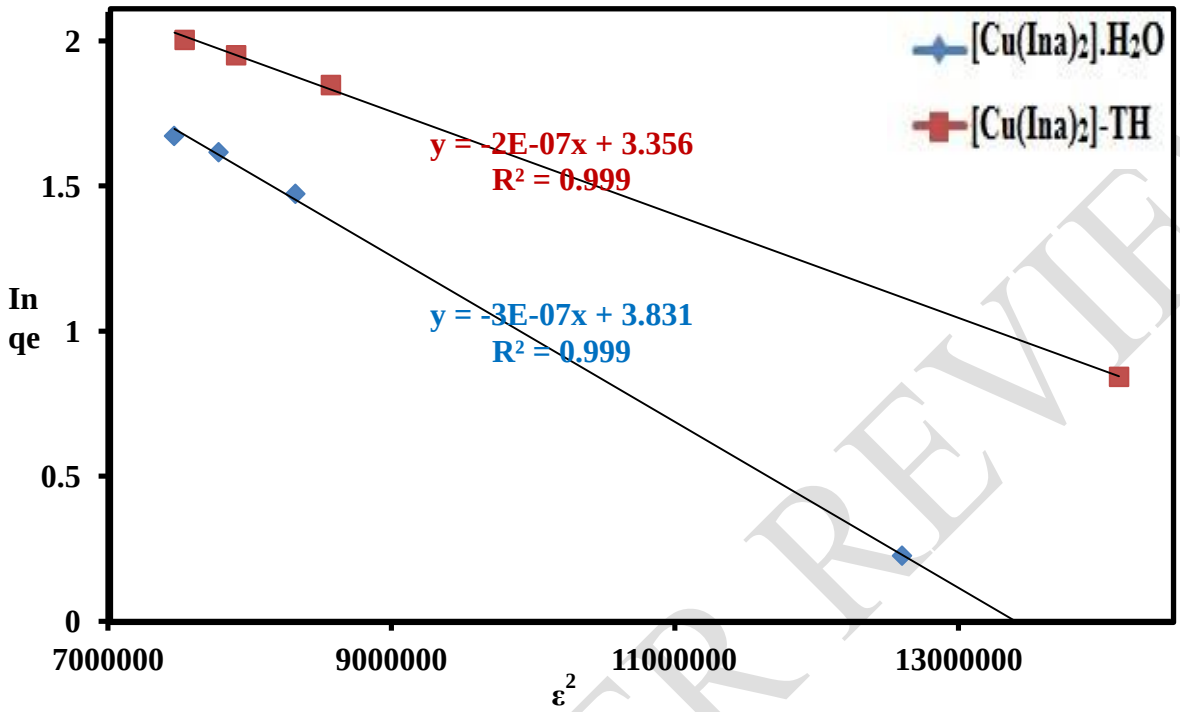

Fig 5: Dubinin–Radushkevich isotherm plot of the Fluorescein adsorption

Table 1: Isotherm parameters with coefficient of determination (R^2) for the adsorption of Fluorescein over [[$Cu(Ina)_2$].H_2O and $[Cu(Ina)_2]$-TH] at 32 ± 2°C.

MOFs	Langmuir Isotherm			Freundlich Isotherm			Temkin Isotherm			Dubinin –Radus. therm			
	Qm (mg/g)	K_L (L/mg)	R^2	Kf (mg/g(L/(L/mg)	N	R^2	b_T	k_T (mg/g)	R^2	q_s (J/mol)	E mg)1/n)	R^2
[Cu(Ina)2].H2O	5.495	0.795	0.960	0.581	1.242	0.969	985	0.678	0.985	46.109	1290	0.999
[Cu(Ina)2]-TH	6.757	3.400	0.983	1.452	1.466	0.988	831	0.984	0.985	28.674	1581	0.999

The regression coefficient values of Langmuir, Freundlich, Temkin and DubininRadushkevich models given in Table 1 indicated that DubininRadushkevich was the most suitable. The isotherms have R^2 values of increasing order Langmuir<Freundlich<Temkin<DubininRadushkevich. The regression coefficient values R^2

show the applicability of the isotherms to the absorption process. It can be seen from Figures 2 – Figure 5 that DubininRadushkevich isotherm has the highest R^2 value of 0.999 and 0.999 for $[Cu(Ina)_2].H_2O$ and $[Cu(Ina)_2]$-TH respectively, therefore, it fits most to the absorption process.

3.9.1.1 EFFECT OF INITIAL CONCENTRATION

The effects of initial dye concentrations were studied at 32± 2^oC for 2 hours using 0.02 g of adsorbent.

As shown in Figures 6, the amount of fluorescein dye adsorbed on $[Cu(Ina)_2].H_2O$ and $[Cu(Ina)_2]$-TH increased with increase in concentration up to 15mg/L and then started to decrease. The effect of the initial dye concentration factor depends on the immediate relation between the dye concentration and the available binding sites on an adsorbent surface. [155] The optimum concentration adsorbed was found to be 5.320 mg/g and 7.412 mg/g for $[Cu(Ina)_2].H_2O$ and $[Cu(Ina)_2]$-TH respectively at a contact time of 2 hours. For the dye, the result implies that at low concentrations of the dye solutions, there still existed unoccupied adsorption sites that got occupied with increase in concentration.[156] At a particular concentration when all the adsorption sites were saturated with dye molecules, the dye molecules started getting desorbed.[157] This accounts for the decrease in the amount of the dye molecules adsorbed from 15mg/L for $[Cu(Ina)_2].H_2O$ and $[Cu(Ina)_2]$-TH. The increase in adsorption capacity with increasing fluorescein dye could be due to higher probability of collision between the adsorbates molecule and the adsorbates surface.[158] The high quantity absorbed of fluorescein dye over $[Cu(Ina)_2]$-TH than $[Cu(Ina)_2].H_2O$ is attributed to acid-base interactions between the basic adsorbate and acidic adsorbent. [136]

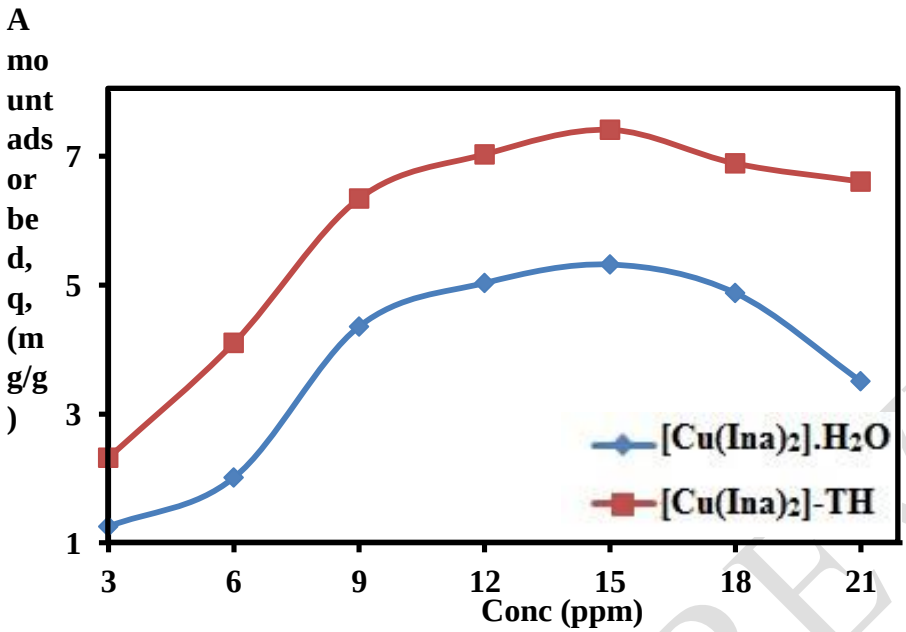

Fig 6: Effect of conc. on the adsorption of fluorescein over $[Cu(Ina)_2].H_2O$ and $[Cu(Ina)_2]$-TH.

3.9.1.2 EFFECT OF CONTACT TIME

The effect of contact time was studied at 32 ± 2^{o}C with 0.02g of adsorbent. The optimum Initial concentrations (i.e. the concentrations at which the highest amount of dye adsorbed were obtained) from the above study were used.

As shown in Figures 7, the optimum time (i.e. the time at which the highest amount of dye adsorbed was obtained) for the adsorption of florescein by $[Cu(Ina)_2].H_2O$ and $[Cu(Ina)_2]$-TH was 180 minutes. The florescein adsorption over $[Cu(Ina)_2].H_2O$ and $[Cu(Ina)_2]$-TH was rapid at the initial stages of the contact period and thereafter it approached to equilibrium. This implies that there were unoccupied sites at 0 - 170 minutes of adsorption that got occupied with time and later attained equilibrium. This shows that there existed a large number of vacant sites for adsorption at the initial stage and they got occupied by the dye molecules but started desorbing with time.[159] As shown in Fig. 7, the adsorbed quantity of florescein is higher in $[Cu(Ina)_2]$TH than $[Cu(Ina)_2].H_2O$ for the whole adsorption time.

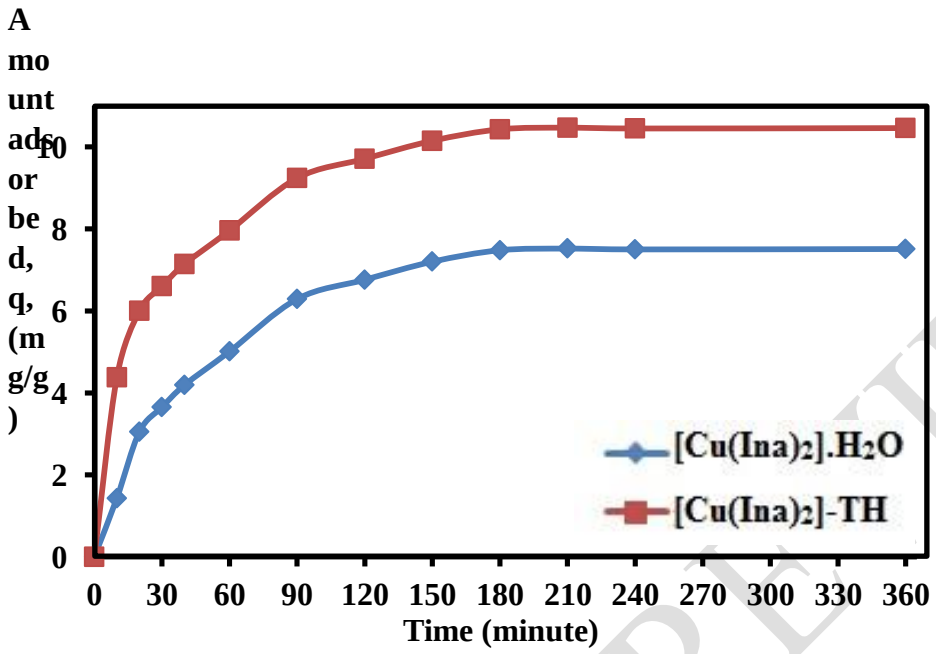

Fig 7: Effect of contact time on the adsorption of florescein over $[Cu(Ina)_2].H_2O$ and $[Cu(Ina)_2]$-TH at initial florescein concentrations of 15 ppm

3.9.1.3 EFFECT OF TEMPERATURE

The effect of temperature was studied using 0.02g of the adsorbents. The results obtained from the above two studies of optimum initial concentration and time were used here. The adsorption of dye usually depends on the temperature of the solution.[160 - 162]

From Figures 8, it can be observed that it was only the adsorption value of florescein on $[Cu(Ina)_2].H_2O$ and $[Cu(Ina)_2]$-TH that increased with temperature up to 45^{o}C. The maximum uptake of 10.852 and 14.027 were adsorbed at temperature of 45^{o}C with $[Cu(Ina)_2].H_2O$ and $[Cu(Ina)_2]$-TH respectively. This result showed that temperature is another factor that can influence the amount of dye adsorbed from solution.

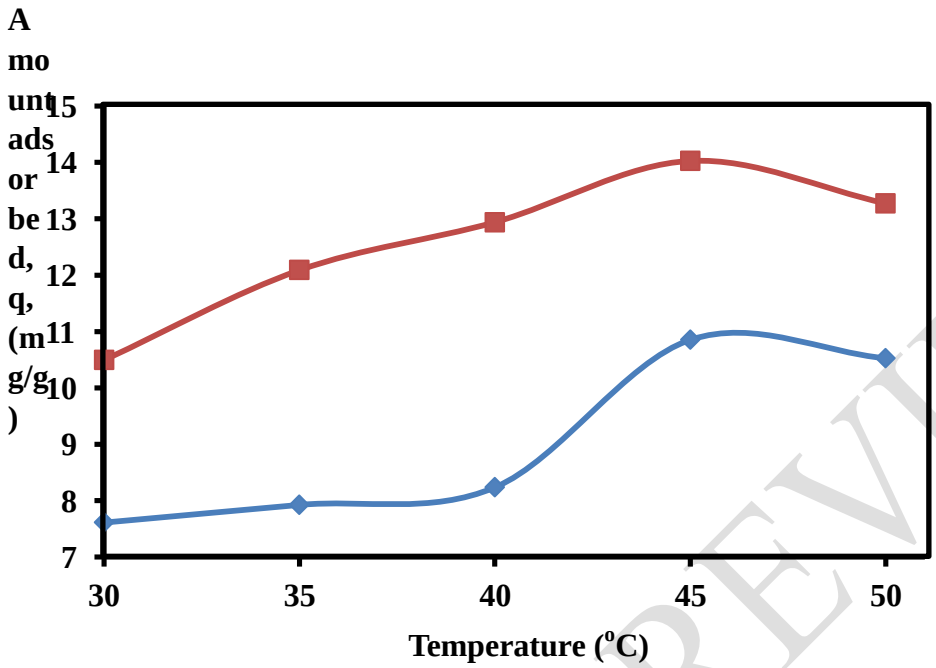

Fig 8: Effect of temperature on the adsorption of florescein over $[Cu(Ina)_2].H_2O$ and $[Cu(Ina)_2]$-TH at initial florescein concentrations of 15 ppm.

3.9.1.5 EFFECT OF pH

The results obtained from the above Three studies of optimum initial concentration, time and temperature were used here.

The adsorption of florescein dye highly depends on the pH of the solution. It is only stable at within pH 7-9, so, the adsorption study of fluorescein dye was carried out at pH values 7 and 9. The amounts of fluorescein dye adsorbed at pH 7 were 49.21 mg/g and 57.742 mg/g for $[Cu(Ina)_2].H_2O$ and $[Cu(Ina)_2]$-TH respectively. This maybe explained with the increased negative charge of the adsorbent in a high pH condition. The two adsorbents ($[Cu(Ina)_2].H_2O$ and $[Cu(Ina)_2]$-TH) exist in the anionic form at pH 9 while fluorescein dye exists in the positive form, therefore, there will be an electrostatic interaction between the dye molecules and the adsorbents.

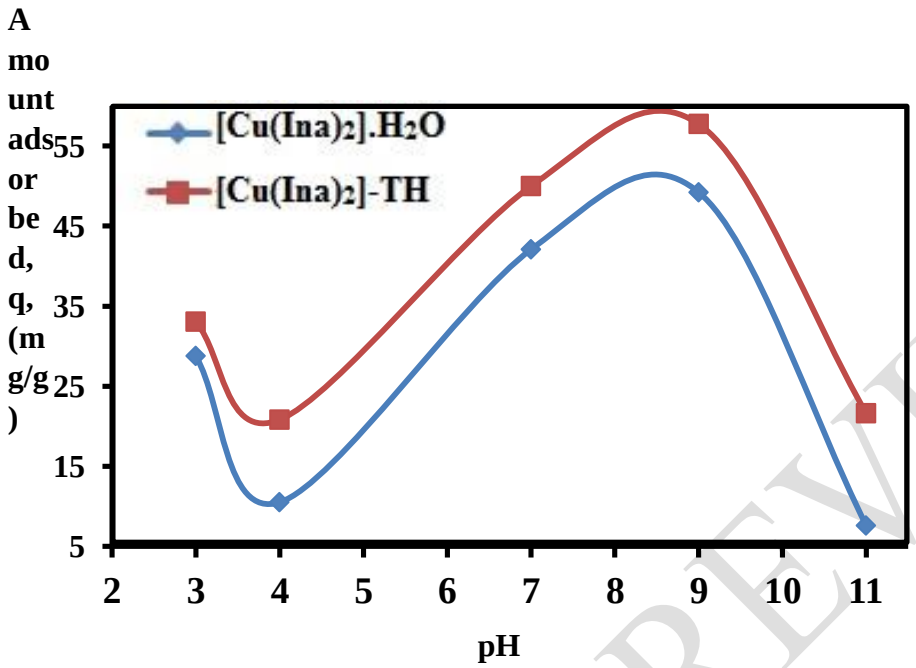

Fig 9: Effect of pH on the adsorption of florescein over $[Cu(Ina)_2].H_2O$ and $[Cu(Ina)_2]TH$ at initial florescein concentrations of 15 ppm.

3.0 RESULTS AND DISCUSSION

3.7. METAL ORGANIC FRAMEWORKS OF THIOGLYCOLIC ACID

Compound were synthesized by the modification of the solvent based method described by Debajyoti*etal*[125]. The solvent-based synthesis of its Compound was carried out in basically ethanol and methanol and all the MOFs show similar coordination point except some in which water coordinate with the metal. During the room temperature synthesis, the starting materials were dissolved in ethanol and methanol and stirred for about two hours at room temperature. Clear solutions of different colours were gotten depending on the metal present and left standing to evaporate slowly. The melting points of the MOFs were different from those of the ligands. Analysis of FTIR and CHN analysis clearly show the formation of the compounds**.** The compounds were insoluble in water and methanol but soluble in solvents having pronounced donor properties e.g. DMSO, DMF and DMA.

All the MOFs were characterized and different results were obtained for the melting point test, IR and elemental analysis. The synthesized compounds have colours which are different from those of the ligands and the melting points of the MOFs are in the range of 100 ^{O}C -250^{O}C which is different from those of the parent ligands.

The physical and analytical data of the MOFs are given in Table 2 below:

Table 2: Physical and Analytical Data of Thioglycolic acid, Some dicarboxylic acid, Nicotinamide and their Cu(II) and Cd(II) MOFs.

Ligand/MOFs	Appearance	Yield (%)	Molecular weight (g/mol)	Melting point (^oC)	Elemental analysis % found (% calculated) C	H	N
Thioglycolic acid	Light yellow liquid	-	92	96	- (26.09)	- (4.35)	- (0.00)
Isonicotinic acid	White powder	-	123	300	- (78.08)	- (4.06)	- (11.38)
Nicotinamide	White powder	-	122	130	- (59.02)	- (4.92)	- (22.95)
[Cu(Thg)(Nic)] (9)	Pale yellow powder	55	275.5	123	39.50 (38.35)	2.20 (2.18)	4.99 (5.08)
[Cu(Ita)(Thg)(H_2O)$_2$] (10)	Brown powder	32	317.5	146	26.42 (26.46)	3.21 (3.15)	<0.10 (0.00)
[Cu(Fum)(Thg)] (11)	Brown powder	69	267.5	205	26.50 (26.92)	1.37 (1.50)	<0.10 (0.00)
[Cu(mal)(Thg)] (12)	Pale yellow powder	54	255.5	112	23.42 (23.48)	1.64 (1.57)	<0.10 (0.00)
[Cd(Oxa)(Thg)(H_2O)$_2$] (13)	Cream powder	58	326.4	153	14.72 (14.71)	1.84 (1.84)	<0.10 (0.00)
[Cd(Ina)(Thg)(H_2O)$_2$] (14)	Cream powder	61	361.4	223	26.54) (26.56)	1.84 (1.66)	4.00 (3.87)

3.7.1 FT-IR Spectroscopy Result of Thioglycolic acid, dicarboxylic acid, Nicotinamide and their MOFs with Cu(II) and Cd(II)

It can be seen from Table 3 and Appendix 1 that FT-IR spectra of the MOFs synthesized are different from those of the ligands. The relevant IR and frequencies of the ligands and the MOFs are presented in Table 3 below:

Table 3: Selected FT-IR absorption band for Thioglycolic acid, Some dicarboxylic acid, Nicotinamide and their Cu(II) and Cd(II) MOFs.

Ligand/MOFs	ν(O-H) (cm^{-1})	ν(N-H) (cm^{-1})	ν(S-H) (cm^{-1})	ν(C=O) (cm^{-1})	ν(C=N) (cm^{-1})	ν(C=C) (cm^{-1})	ν(C-O) (cm^{-1})	ν(C-S) (cm^{-1})	ν(M-O) (cm^{-1})
Thioglycolic acid	3200br	-	2569w	1716s	-	-	1298s	671w	-
Fumaric acid	3417br	-	-	1674s	-	1427m	1274s	-	-
Isonicotinic acid	3437br	-	-	1716s	1616m	1564m	1028s	-	-
Nicotinamide	-	3367m 3163m	-	1710m	1681m	1620m 1595m	-	-	-
[Cu(Thg)(Nic)] (9)	-	3404m 3184m	2397w	1708m	1678m	1602m	1201s	688w	443w
[Cu(Ita)(Thg)(H_2O)$_2$] (10)	-	-	2364w	-	-	1645m	1141s	707w	426w
[Cu(Fum)(Thg)] (11)	-	-	2364w	1734m	-	1616m	1197s	682w	486w
[Cu(mal)(Thg)] (12)	-	-	2372w	1627m	-	-	1118s	696w	399w
[Cd(Oxa)(Thg)(H_2O)$_2$] (13)	-	-	2364w	1614m	-	1456m 1440m	1224s	715w	501w
[Cd(Ina)(Thg)(H_2O)$_2$] (14)	-	-	2364w	-	1116m	1552m	1226s	707w	453w

br= broad, m= medium, s= strong, sh= sharp, w= weak

The infrared spectra of the MOFs in the far IR region 4,000 – 400 cm^{-1} were compared with those of the ligands as shown in Table 4. The infra-red spectra of the MOFs were found to be different from those of the ligand and showed either a shift or disappearance of some characteristic frequencies and appearance of some new frequencies. The carboxylate protons were all deprotonated in all the carboxylate acids present. Carboxylic acid always have coordination sites at only the carboxylic acid functional groups, Nicotinamide is an amide having coordination sites at different functional groups (C=N and C=O) while Thioglycolic acid is a thiol having coordination site at different functional groups (H-S, O-H and C=O). From table 4 above, peaks characteristics of various ligands are obtained in the spectra of the MOFs, an indication that the ligands are coordinated to the metal ion. The broad band at 3068 cm^{-1}(due to the O-H) present in thioglycolic and dicarboxylic acid disappeared in MOFs all the MOFs, this is

an indicative of the deprotonation and coordination through the O-H group.[145] These NH bands in the MOFs are split and appear in the 3450–3150 cm^{-1} region at higher wave number than comparable bands in free nicotinamide because of hydrogen bonding. The absorption bands of the ν(C-O) shifted from their initial bands for all the MOFs. This clearly indicates a bidentate mode of O^- in this MOF indicating that the bicarboxtlate ions function as bridging moieties. [152]

3.7.2 Proposed Structures of the MOFs of Thioglycolic Acid

From the analytical data and the spectroscopic studies, it was found that the Copper ion coordinates via the nitrogens of the amide & pyridine ring in the Nicotinamide, oxygen of the hydroxyl group & sulphur on the thiol group in thioglycolic acid and oxygen of the hydroxyl group in dicarboxylic acid to form a tetrahedral compound mainly while some have two molecule of water inside the coordination sphere to make them octehedral.

3.8. THIOL-FUNCTIONALIZATION OF THE SYNTHESIZED MOFS

Thiol-functionalizations of the MOFs were carried out as described in the experimental section. Each of the MOFs was modified chemically by Thiolation as previously described by Ling-Guang *et al.*[124] After modification with acidic functional group all the MOFs undergo significant change both physical and chemical. The colour, texture and melting point of the modified MOFs were totally different from those as-synthesized. The change in the chemical composition of the MOFs as thiolation was confirmed by CHN, FT-IR and XRPD.

3.8.1 *THIOLATION of [Cu(INA)$_2$]*

The thiolation of ***[Cu(INA)$_2$]*** was carried out by refluxing ***[Cu(INA)$_2$]*** with thioglycolic acid at 80 ^oC. Analysis of XRPD, FTIR and CHN analysis clearly shows the thiolation of ***[Cu(INA)$_2$].*** The elemental analysis (CHN), XRPD and FT-IR spectra data obtained for the functionalized ***[Cu(INA)$_2$]*** was compared with that of the unfunctionalized and it can be inferred from the results that the functionalization was successful.

Table 4: FT-IR band frequencies of *[Cu(INA)$_2$]* and thiol-modified *[Cu(INA)$_2$]* MOFs

MOFs	ν(O-H) (cm^{-1})	ν(S-H) (cm^{-1})	ν(C=O) (cm^{-1})	ν(C=N) (cm^{-1})	ν(C=C) (cm^{-1})	ν(C-O) (cm^{-1})	ν(C-S) (cm^{-1})	ν(M-N) (cm^{-1})	ν(M-O) (cm^{-1})
[Cu(INA)$_2$]	3460br	-	1722m	1550m	1419m	1232s	-	578w	457w
[Cu(INA)$_2$]-TH	-	2366	1734m	1612m	1436m	1290s	821w	617w	505w

The above shows FT-IR data of the thiol-functionalized samples, as well as the unfunctionalized [Cu(INA)$_2$] powered. The functionalized [Cu(INA)$_2$] shows most of the bands on the unfunctionalized [Cu(INA)$_2$] have shifted to higher wave number. The bands around 2366 and 821 cm^{-1} observed in thiol functionalized samples can be attributed to the presence of ν (S– H) and ν (C–S) vibrations respectively indicating the presence of thioglycolic acid. Although the peak at 2366 cm^{-1} corresponding to ν(S–H) is not very strong, obvious shift of the aliphatic ν(C–H) stretching vibrations at 2800–3000 cm^{-1} to larger values was found, as observed when the molecule is coordinated to a Lewis acid center[153, 154]. The result clearly reveals that thioglycolic acid molecule(s) were successfully grated onto the UMCs in channels created in the framework, rather than adsorbed on external surface of [Cu(INA)$_2$].

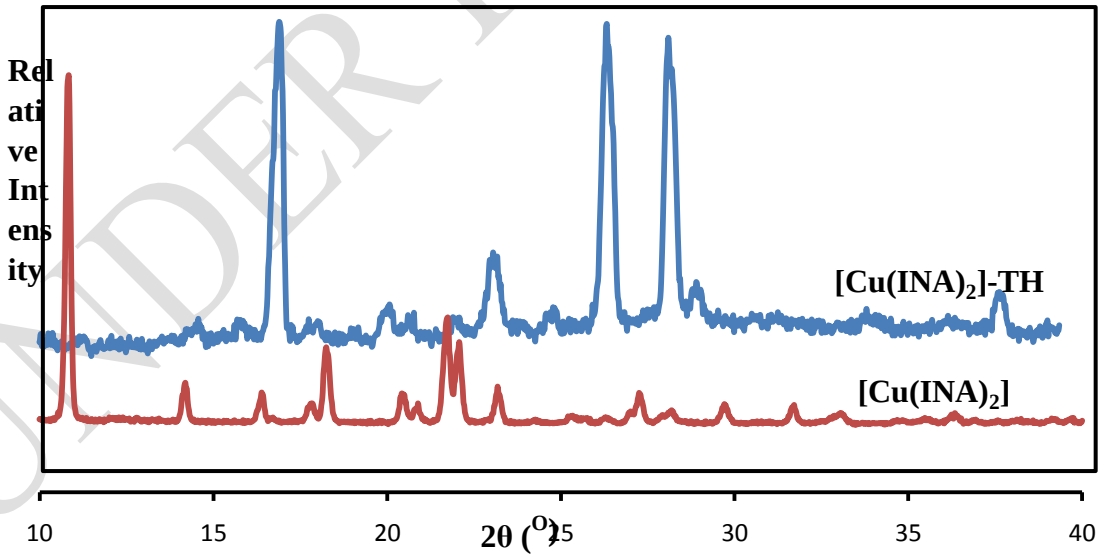

Fig. 10: XRPD pattern of *[Cu(INA)$_2$]* and thiol-modified *[Cu(INA)$_2$]*

It can be observed in Figure 10 that the XRPD of the as-synthesized [Cu(INA)$_2$] differ from that of the thiol-functionalized [Cu(INA)$_2$], this is an evidence of modification of product. High intensity Bragg diffraction peaks are observed at 10.22^O, 20.84^O and 21.92^{O}with low intensity peaks at 13.66^O 15.98^O, 17.78^O, 18.26^O, 20.14^O and 26.84^O for as-synthesized [Cu(INA)$_2$] while High intensity Bragg diffraction peaks are observed at 16.92^O, 26.33^O and 28.09^{O}with low intensity peaks at 13.66^O, 14.59^O, 15.90^O, 20.17^O, 21.76^O, 23.05^O, 24.82^O and 28.91^O for thiol-functionalized [Cu(INA)$_2$]. The observed XRPD pattern of the functionalized *[Cu(INA)$_2$* obtained in the solvent based reaction was totally different form that of the unfunctionalized [Cu(INA)$_2$] which confirmed the successful functionalization of [Cu(INA)$_2$].

3.8.6. *THIOLATION of* [Cu$_3$(BTC)$_2$]

The thiolation of **[Cu$_3$(BTC)$_2$]**was carried out by refluxing **[Cu$_3$(BTC)$_2$]**with thioglycolic acid at 150 ^{o}C. Analysis of FTIR and CHN analysis doesn‘t shows the thiolation of **[Cu$_3$(BTC)$_2$].**The elemental analysis (CHN) and FT-IR spectra data obtained for the functionalized **[Cu$_3$(BTC)$_2$]** was compared with that of the unfunctionalized **[Cu$_3$(BTC)$_2$]** and it can be inferred from the results that the functionalization was unsuccessful.

3.9 ADSORPTION OF FLORESCEIN DYES ON THE AS-SYNTHESIZED AND THIOL FUNCTIONALIZED [Cu(Ina)$_2$].H$_2$O

Dye products correspond to a number of chemical compositions/constituents, which are widely used in our everyday life. Several research works have demonstrated the presence of dye in the effluent of wastewater treatment plants, rivers, lakes and occasionally, ground water. In the previous sections, the effect of the discharge of effluents from textile, paper, printing and dyestuff industries have been discussed. Also, various means of environmental remediation and the drawbacks of each of these techniques were given, thus the need for adsorptive techniques for the removal of these effluents. MOFs have been proven to be effective adsorptive materials due to the properties they possess i.e. large pores and surface area which make them better off than the existing adsorbents. Out of the synthesized MOFs reported,[Cu(Ina)$_2$].H$_2$Ois a known MOFs and was functionalized used as an adsorbent for the adsorption of fluorescein dye.

Here, the adsorption of fluorescein dye onto as-synthesized and thiol functionalized $[Cu(Ina)_2].H_2O$ was carried out and reported. The objective of this section was to investigate the possible use of the synthesized MOFs as an alternative adsorbent material for the removal of fluorescein dyes from aqueous solution and to see if thiol functionalized $[Cu(Ina)_2].H_2O$ will adsorb better that the unfunctionalized $[Cu(Ina)_2].H_2O$.

3.11 CONCLUSION

Metal Organic frameworks and metal complexes constructed from Zn(II), Cu(II) and Ni(II); and carboxylic acids (Fumaric acid, Glutaric acid, Isonicotinic acid, Terephtalic acid, Thioglycolic acid and Trimesic acid) have been synthesized using mechanochemical and room temperature solvent- based methods. The compounds obtained from both methods were characterized using elemental analysis, FT-IR spectroscopy and XRPD. The results showed that the good products were obtained. It was discovered that most these carboxylate ligands coordinated to the metals in a bidentate fashion thereby exhibiting tetrahedral geometry for MOFs.

Six of the synthesized MOFs were functionalized (with thioglycolic acid) using Solvent- based methods, but just five of the functionalization was successful. The compounds obtained from the thiolation were characterized using elemental analysis, FT-IR spectroscopy and XRPD. The results showed that the products form were totally different from that of the as-synthesized - MOFs. ($[Cu(Ina)_2].H_2O$ and $[Cu(Ina)_2]$-TH).

. This research on metal-organic frameworks (MOFs) for dye removal from water is a vital advancement in environmental remediation. It aligns with themes of predictive analysis in resource management (11), highlighting the importance of comprehensive strategies in complex challenges (12). The principles of data-driven decision-making (13) and the significance of organizational culture in fostering innovation (14) are also applicable in the development and implementation of MOFs. Additionally, the need for foundational groundwork in technology development (15) parallels the research efforts required for effective MOF applications in environmental solutions.

3.12 RECOMMENDATION

It is recommended that further analytical methods such as BET analysis to determine the pore sizes of the adsorbents, thermogravimetris analysis, NMR and mass spectroscopies should be done to further elucidate the morphologies and porosity of the thio-functionalized MOFs. More researches should be done on the functionalization of MOFs using other functionalizing agent most especially Copper trimasate which has show a negative result with thiolation. Also, more researches should be done on other applications of MOFs, most especially in military and security sector on how it can be used for loading and detecting of explosive.

REFERENCES

1. Kinoshita Y., Matsubara I., Higuchi T., Saito Y.; (1959): The Crystal Structure of Bis(adiponitrilo)copper(I) nitrate, Bull. Chem. Soc. Jpn. 32, 1221–1226. doi: 10.1246/bcsj.32.1221.
2. Tomic, E.A.; (1965): Thermal Stability of Coordination Polymers. J. of Appl. Polymer Sci., 9(11), 3745-3748.
3. Yaghi O. M., Li H.; (1995): Hydrothermal Synthesis of a Metal- Organic Framework Containing Large Rectangular Channels. J. Am. Chem. Soc. 117, 10401–10402. doi: 10.1021/ja00146a033.
4. Eddaoudi M., Moler O.B., Li H,, Chen B,, Reinekee T.M,, O'Keeffe M,, Yaghi O. M,; (2001): Secondary Building Units as A Basis For The Design Of Highly Porous And Robust Metal-Organic Carboxylate Frameworks. Acc. Chem. Res. 34: 319-330
5. TrenchemontaaneD,J, Mendoza-Cortes J.L,, O'Keeffe M. and Yaghi O.M, (2009): Secondary Building Units, Nets And Bonding In The Chemistry Of Metal-Organic Frameworks. Chem Soc Rev. 378,1257-1283.
6. Kitagawa S, Kitaura R., Noro S,(2004): Functional Porous Coordination Polymers. AngewChemInt Ed.,43,2334-2375.
7. Eddaoudi, M.; Kim, J. Rosi, N. L.; Vodak, D. T.; Wachter, J.; O'keeffe, M and Yaghi, O. M. (2002): Systematic Design Of Pore Size And Functionality In IsoreticularMetalOrganic Frameworks and Application in Methane storage. Sci., 295, 469 – 472.

8. Ferey G.; (2008): Hybrid Porous Solids: Past, Present, Future. Chem Soc Rev. 37,191214.
9. Eddaoudi L.H, O'Keeffe M, Yaghi M, (1999): Design and Synthesis of an Exceptionally Stable and Highly Porous Metal-Organic Framework. Nature (London), 402, 276.
10. Defination of porous by the free online. dictionary. http.//dictionary.reference.com/browse/porous. (retrived on 25/11/2013).
11. Omogoroye, O. O., Olaniyi, O. O., Adebiyi, O. O., Oladoyinbo, T. O., & Olaniyi, F. G. (2023). Electricity Consumption (kW) Forecast for a Building of Interest Based on a Time Series Nonlinear Regression Model. Asian Journal of Economics, Business and Accounting, 23(21), 197–207. https://doi.org/10.9734/ajeba/2023/v23i211127
12. Olaniyi, O. O., Okunleye, O. J., Olabanji, S. O., Asonze, C. U., & Ajayi, S. A. (2023). IoT Security in the Era of Ubiquitous Computing: A Multidisciplinary Approach to Addressing Vulnerabilities and Promoting Resilience. Asian Journal of Research in Computer Science, 16(4), 354–371. https://doi.org/10.9734/ajrcos/2023/v16i4397
13. Olaniyi, O. O., Shah, N. H., &Bahuguna, N. (2023). Quantitative Analysis and Comparative Review of Dividend Policy Dynamics within the Banking Sector: Insights from Global and U.S. Financial Data and Existing Literature. Asian Journal of Economics, Business and Accounting, 23(23), 179–199. https://doi.org/10.9734/ajeba/2023/v23i231180
14. Olaniyi, O. O., Asonze, C. U., Ajayi, S. A., Olabanji, S. O., & Adigwe, C. S. (2023). A Regressional Study on the Impact of Organizational Security Culture and Transformational Leadership on Social Engineering Awareness among Bank Employees: The Interplay of Security Education and Behavioral Change. Asian Journal of Economics, Business and Accounting, 23(23), 128–143. https://doi.org/10.9734/ajeba/2023/v23i231176
15. Oladoyinbo, T. O., Adebiyi, O. O., Ugonnia, J. C., Olaniyi, O. O., & Okunleye, O. J. (2023). Evaluating and Establishing Baseline Security Requirements in Cloud Computing: An Enterprise Risk Management Approach. Asian Journal of Economics, Business and Accounting, 23(21), 222–231. https://doi.org/10.9734/ajeba/2023/v23i211129

APPENDIX 1

1. FT-IR SPECTRA OF MECHANOCHEMICALLY SYNTHESIZED MOFs.

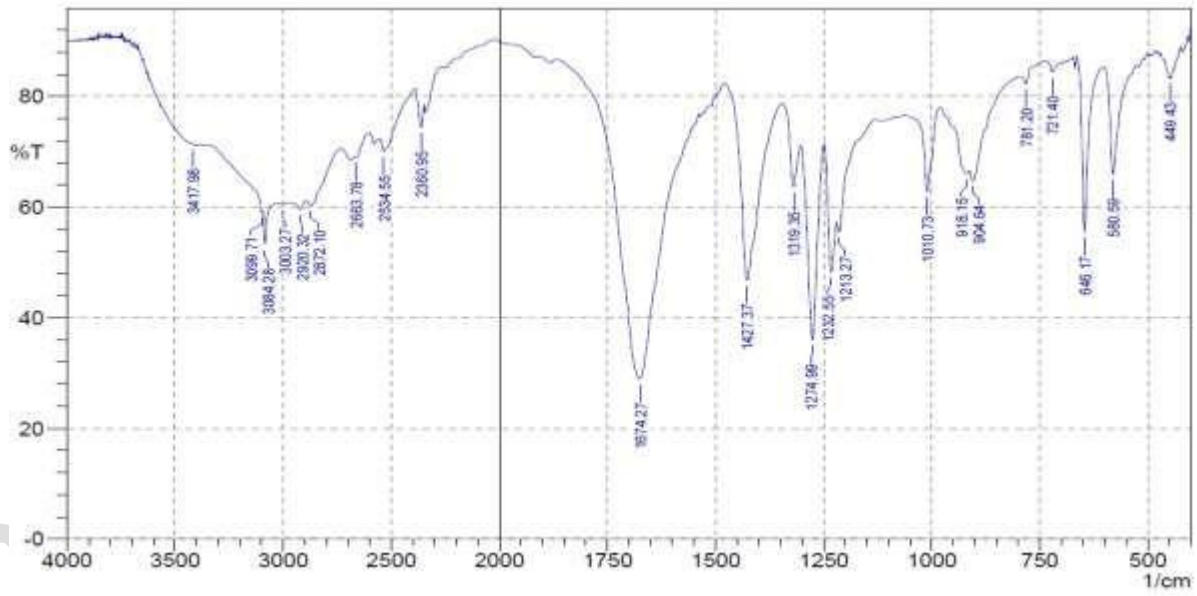

FT-IR spectrum of Fumaric acid

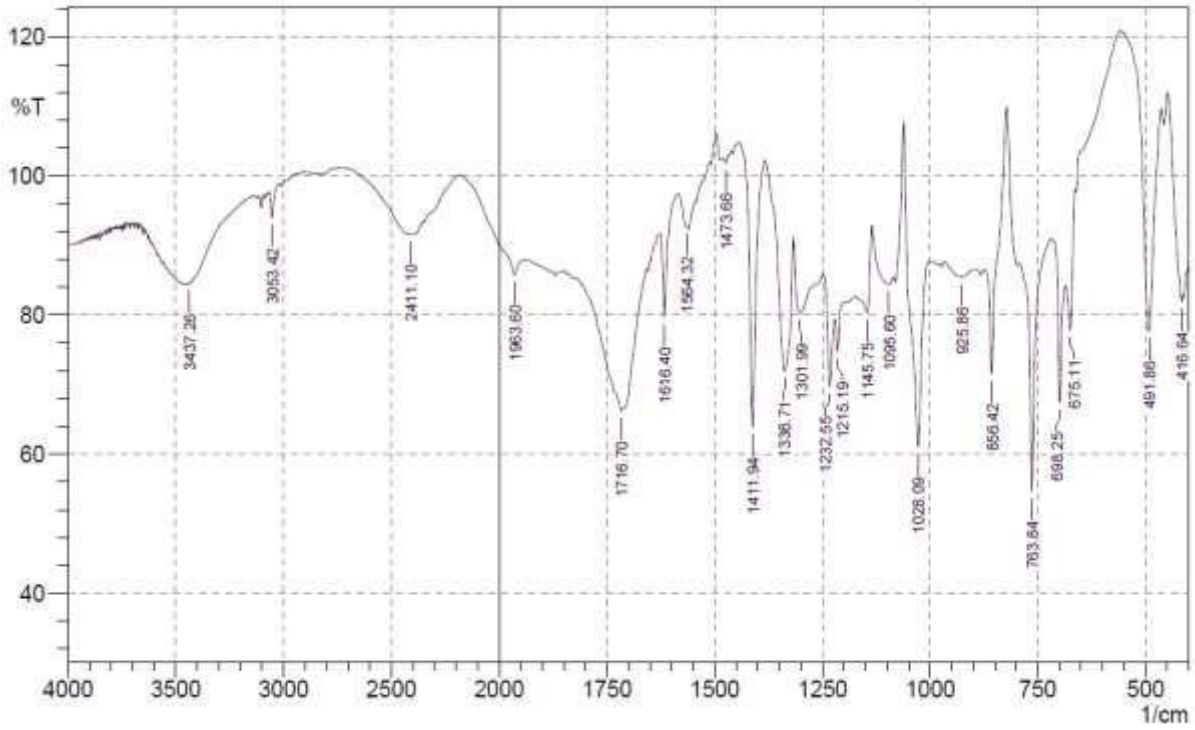

FT-IR spectrum of isonicotinic acid

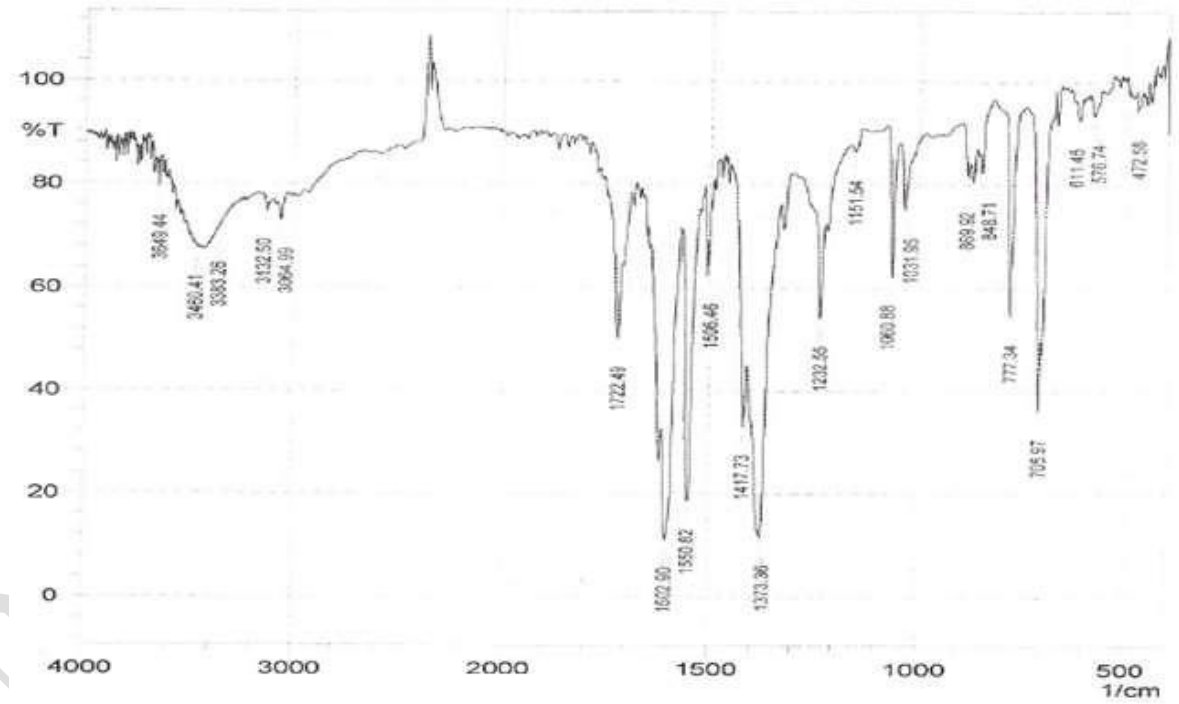

FT-IR spectrum of $[Cu(Ina)_2].H_2O$

6. FT-IR SPECTRA OF ZINC FUMARATE AND ITS DERIVATIVE..

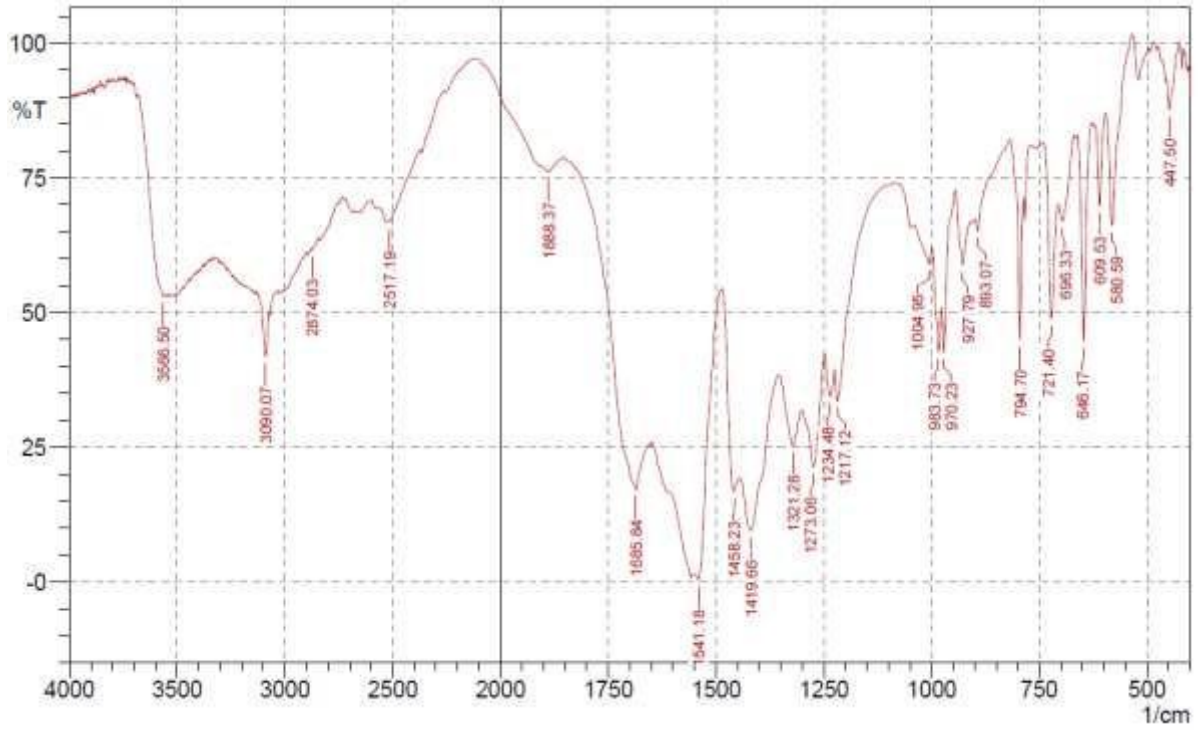

FT-IR spectrum of $[Zn(Fum)(H_2O)_2]$

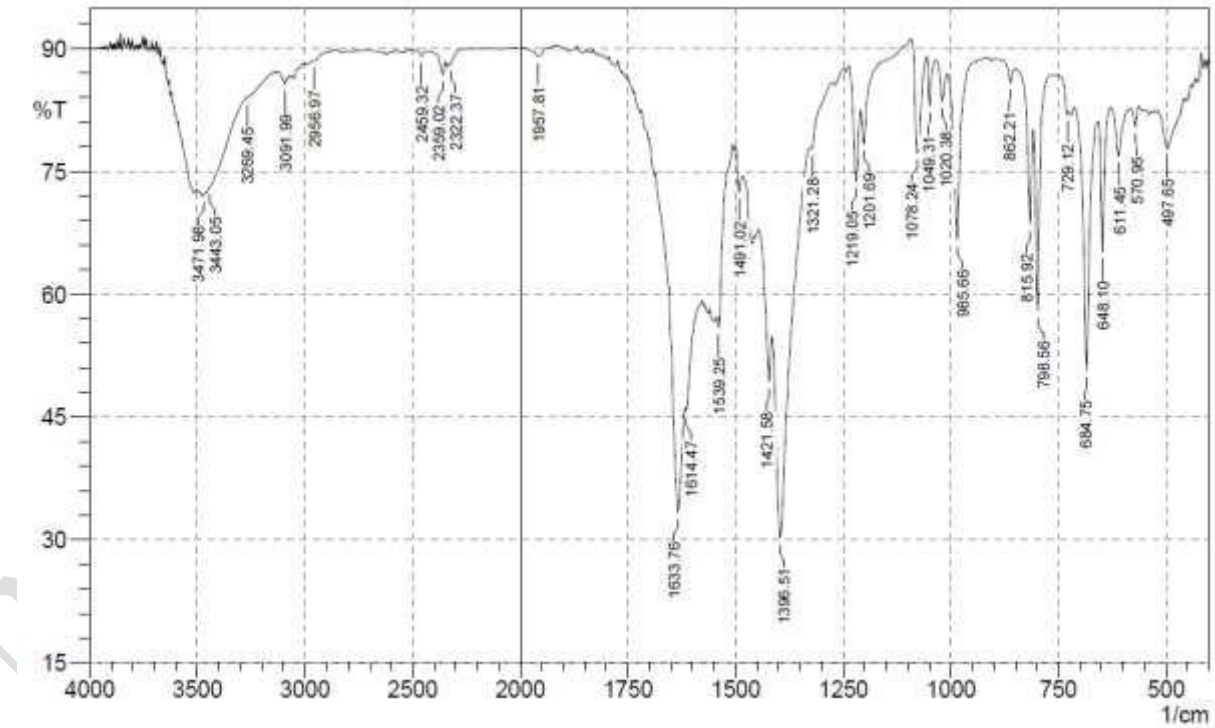

FT-IR spectrum of $[Zn_2(Fum)_2(bpy)]$

2. FT-IR SPECTRA OF SOLVENT-BASED SYNTHESIZED MOFs.

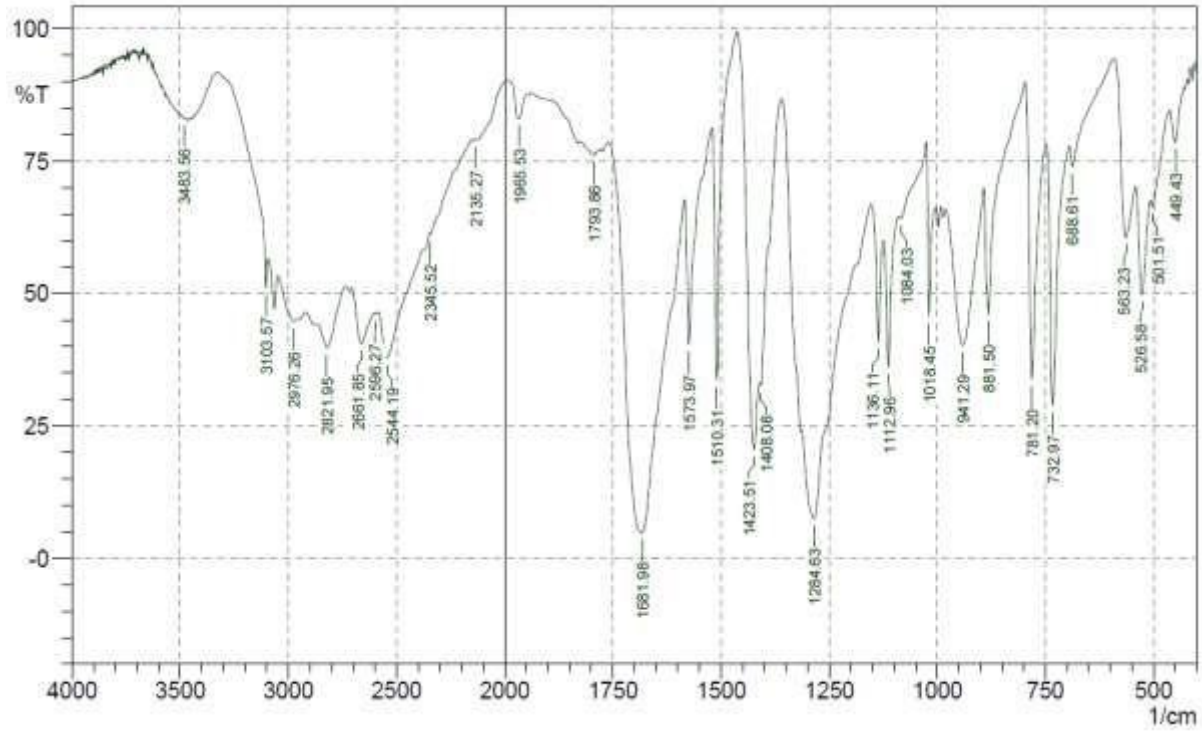

FT-IR Spectrum of Terephthalic acid.

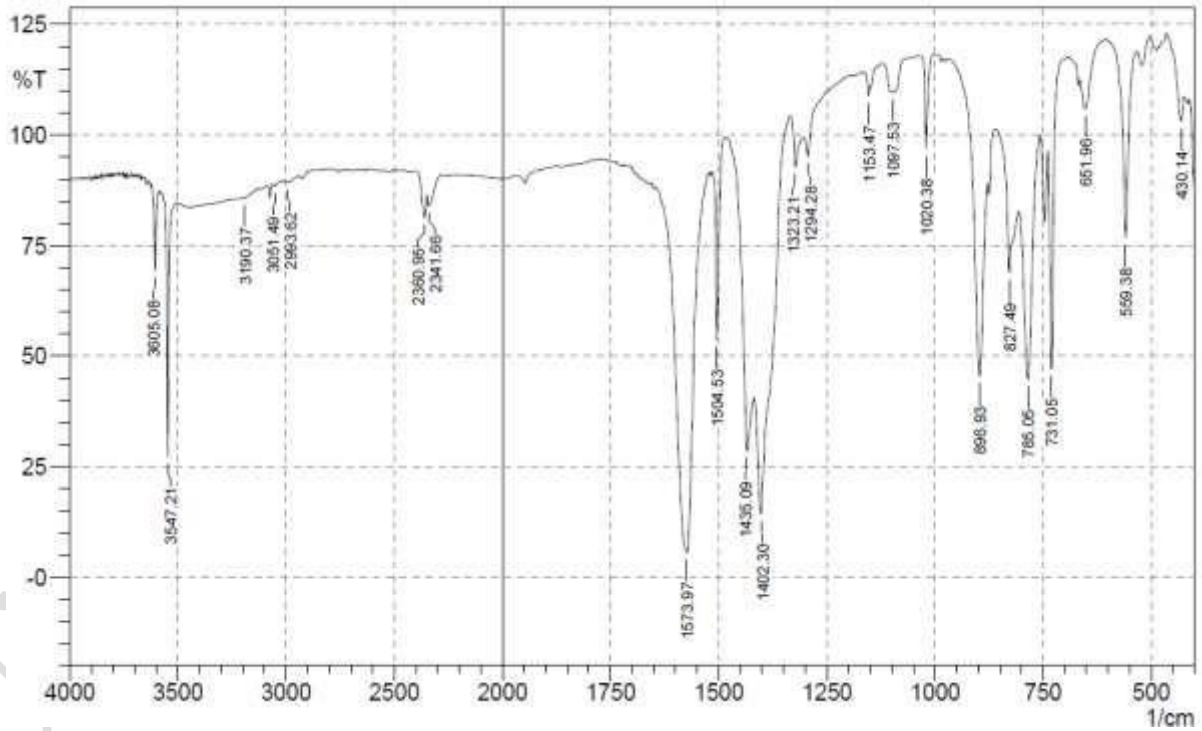

FT-IR spectrum of $[ZnO_4(BDC)_3]$

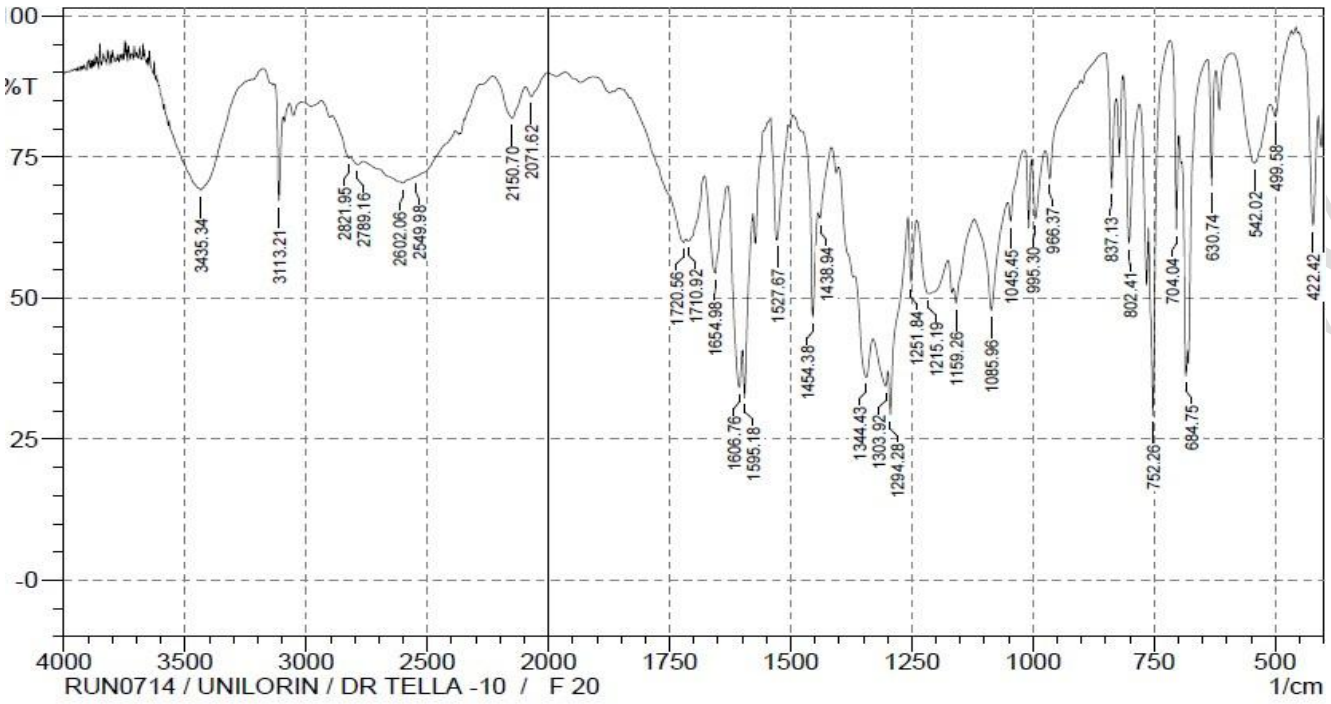

FT-IR spectrum of trimesic acid

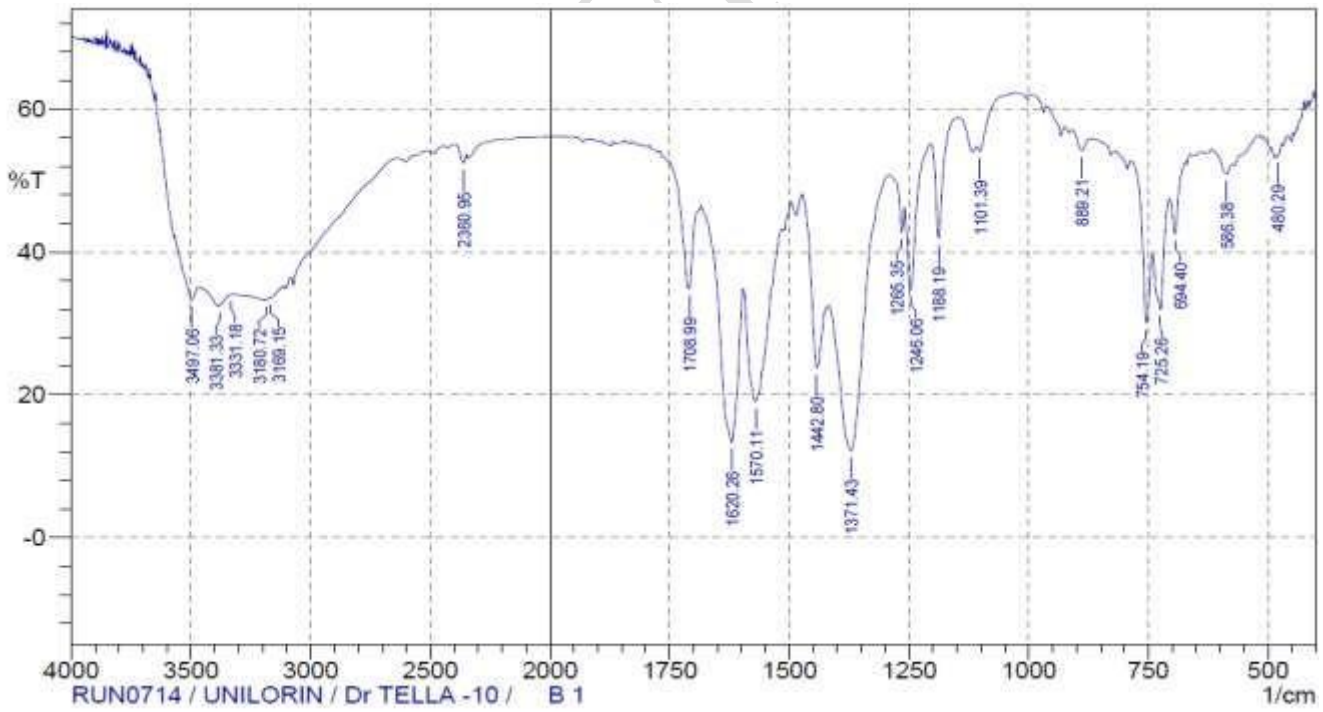

FT-IR spectrum of [Cu_3 (BTC) $_2$]

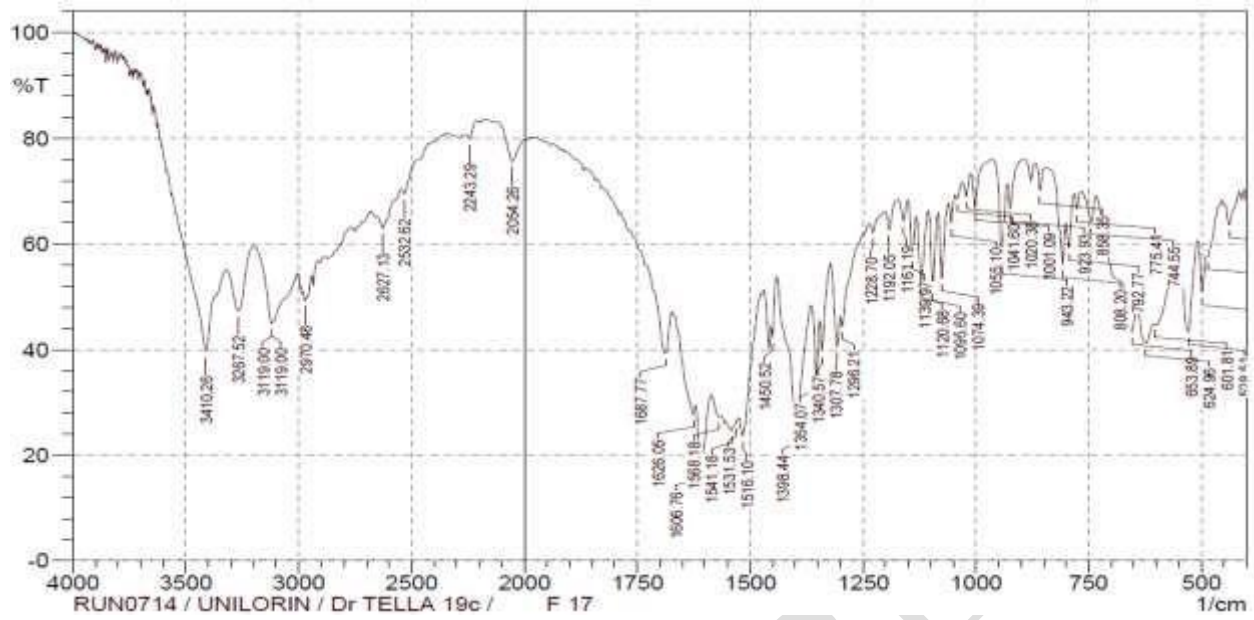

FT-IR of Glutaric acid

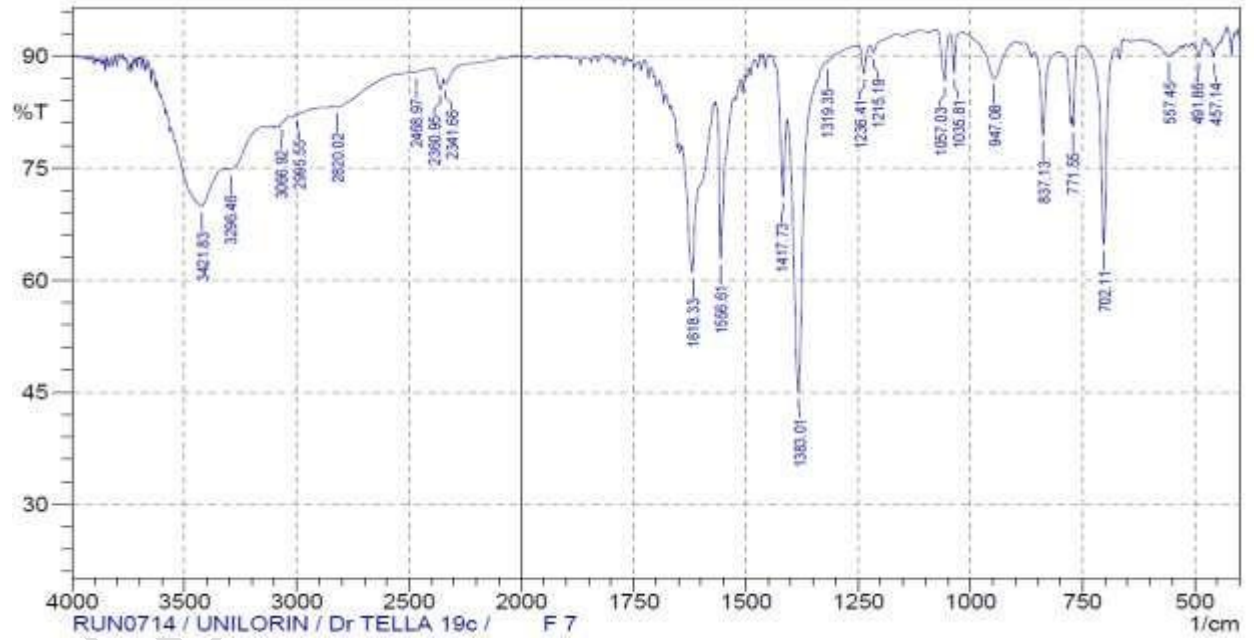

FT-IR of [(Cu(Ina)(Glut)$(H_2O)_2$]

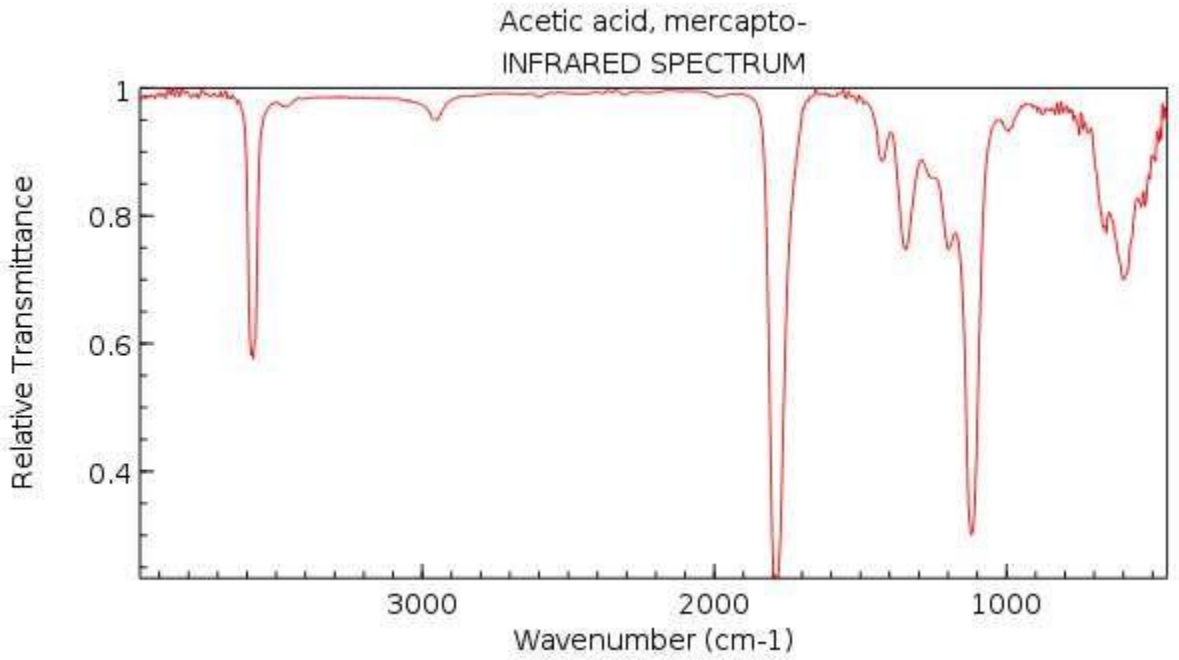

FT-IR of Thioglycolic acid

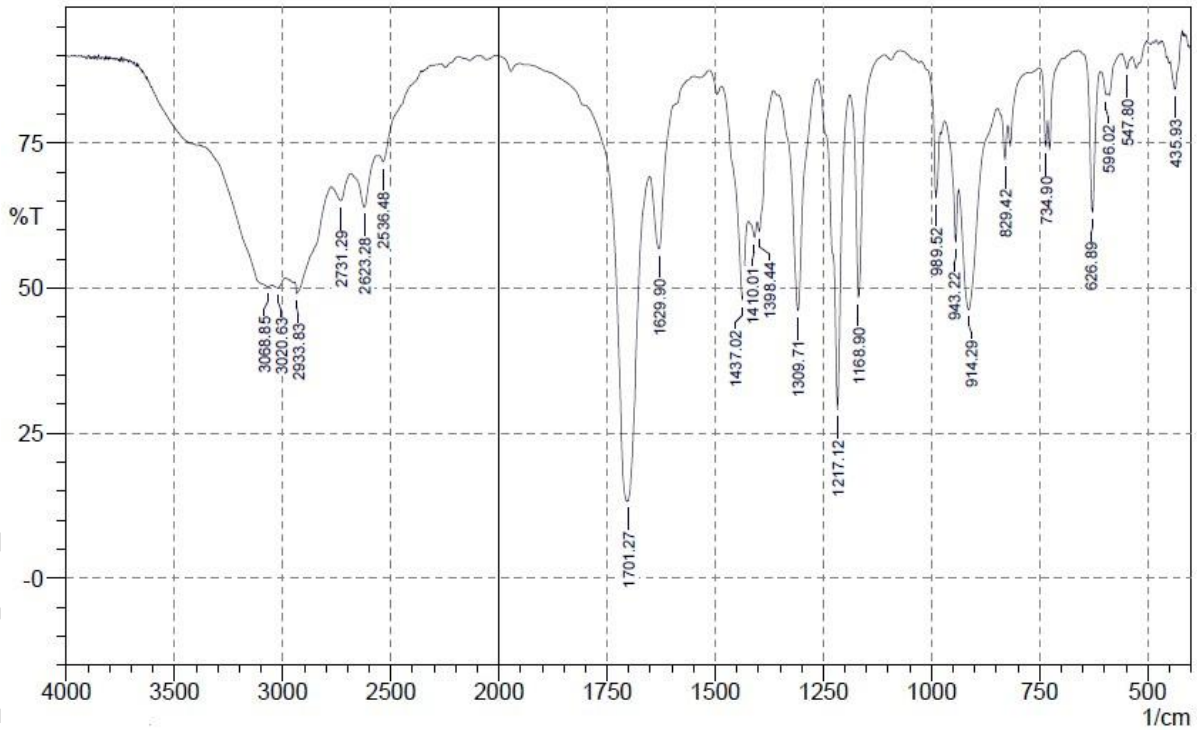

FT-IR spectrum of Itaconic acid

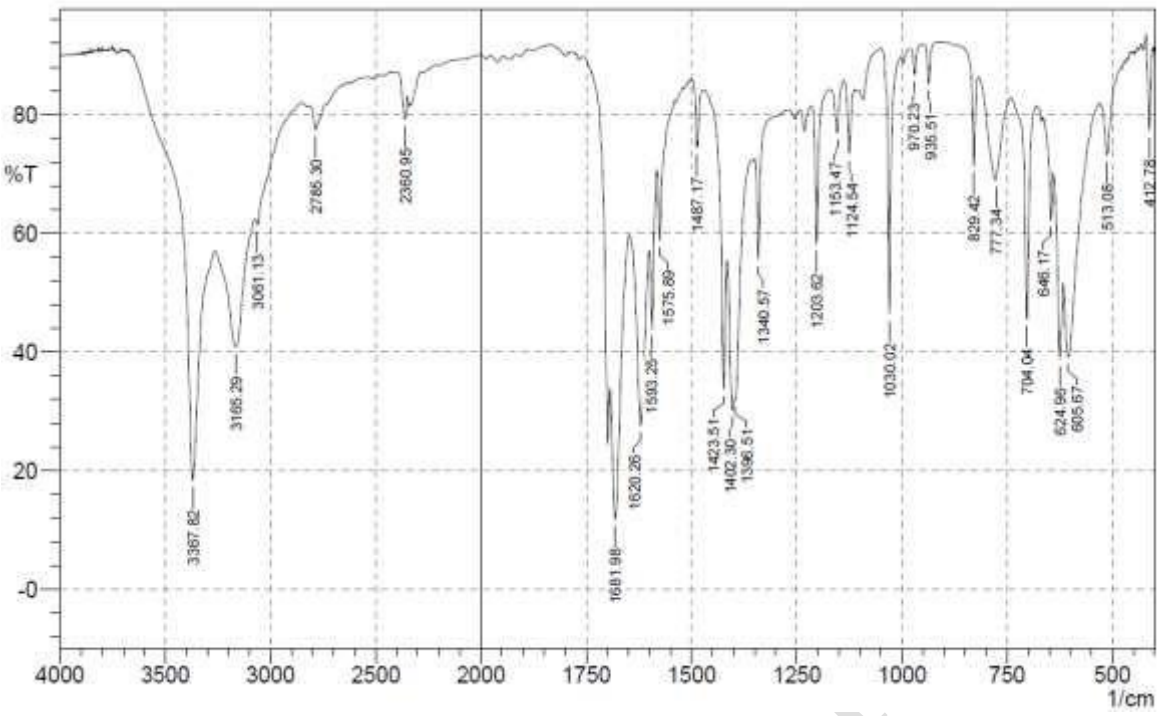

FT-IR spectrum of Nicotinamide

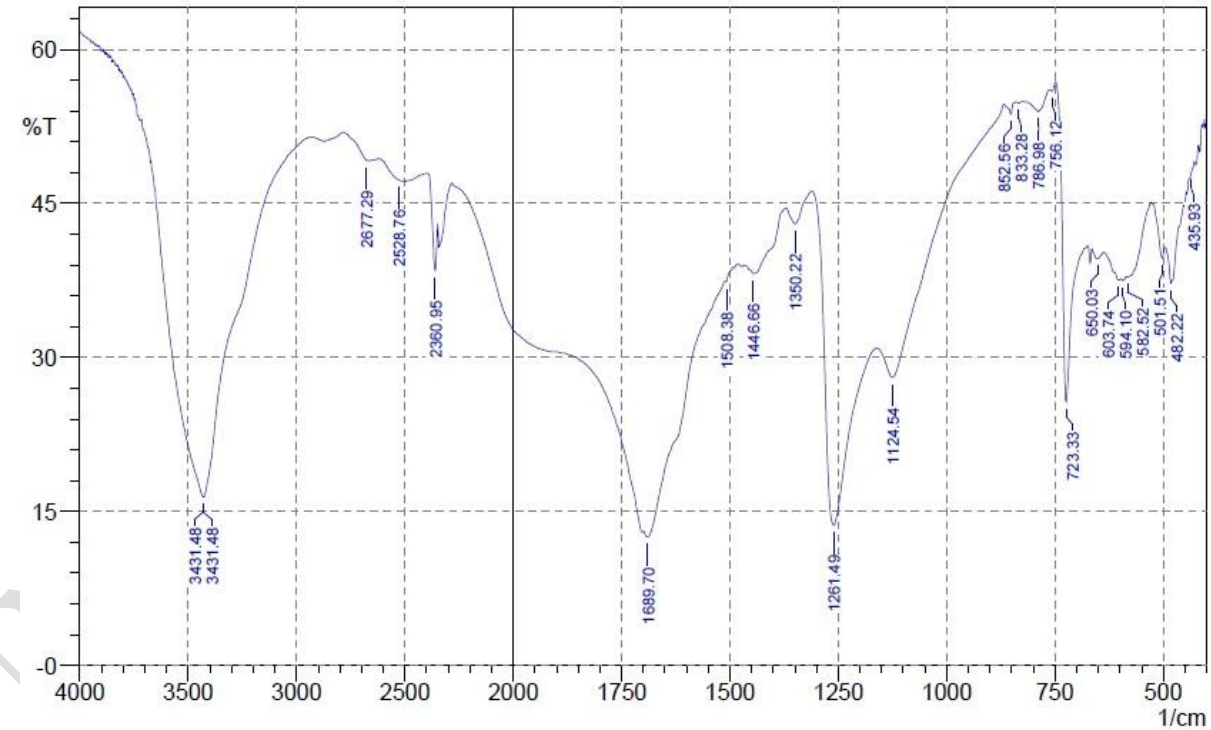

FT-IR spectrum of Oxalic acid

.

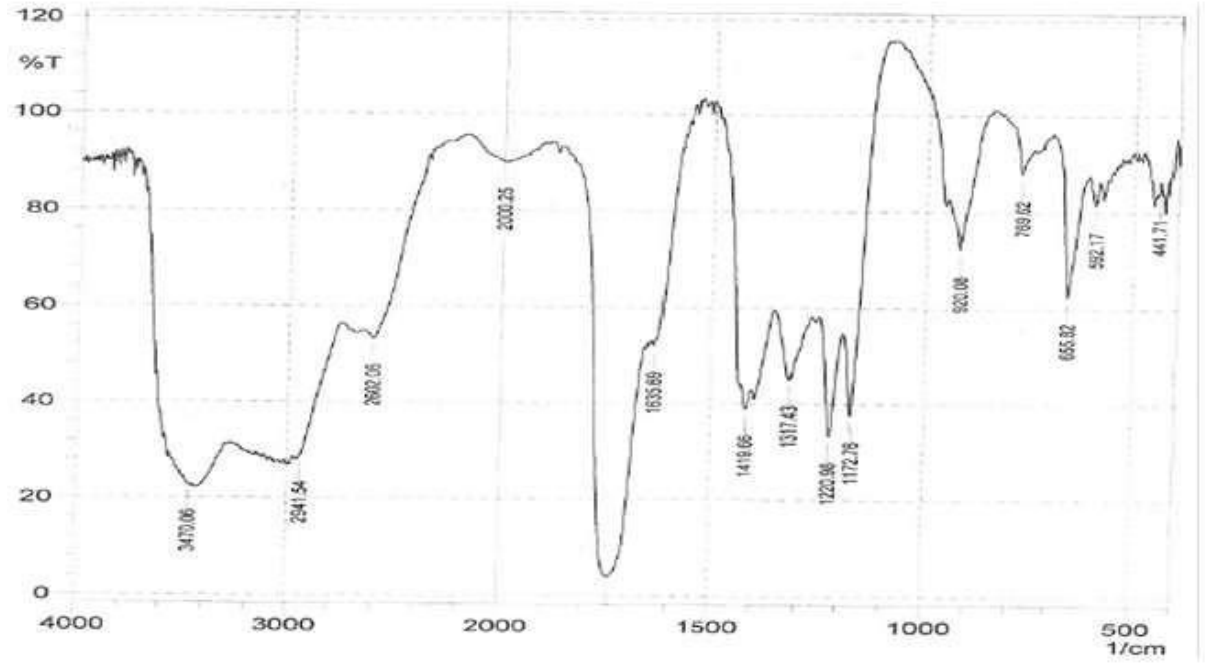

FT-IR spectrum of Malonic acid

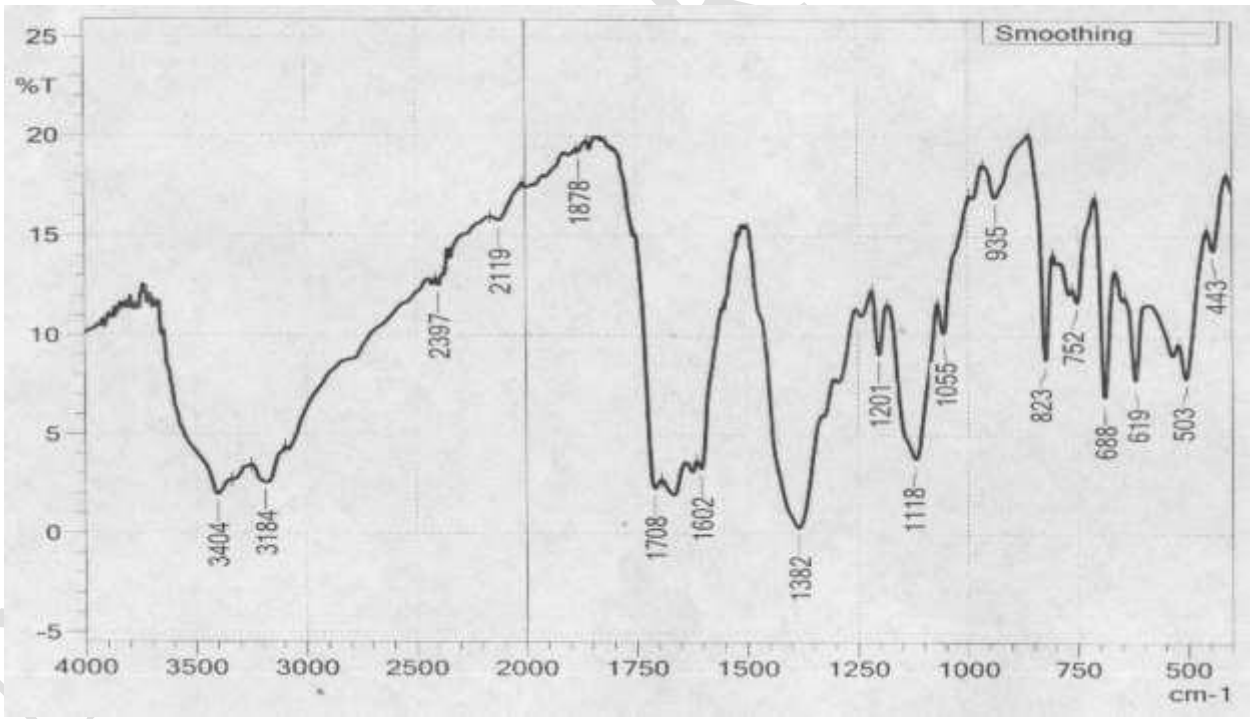

FT-IR spectrum of [Cu(Thg)(Nic)]

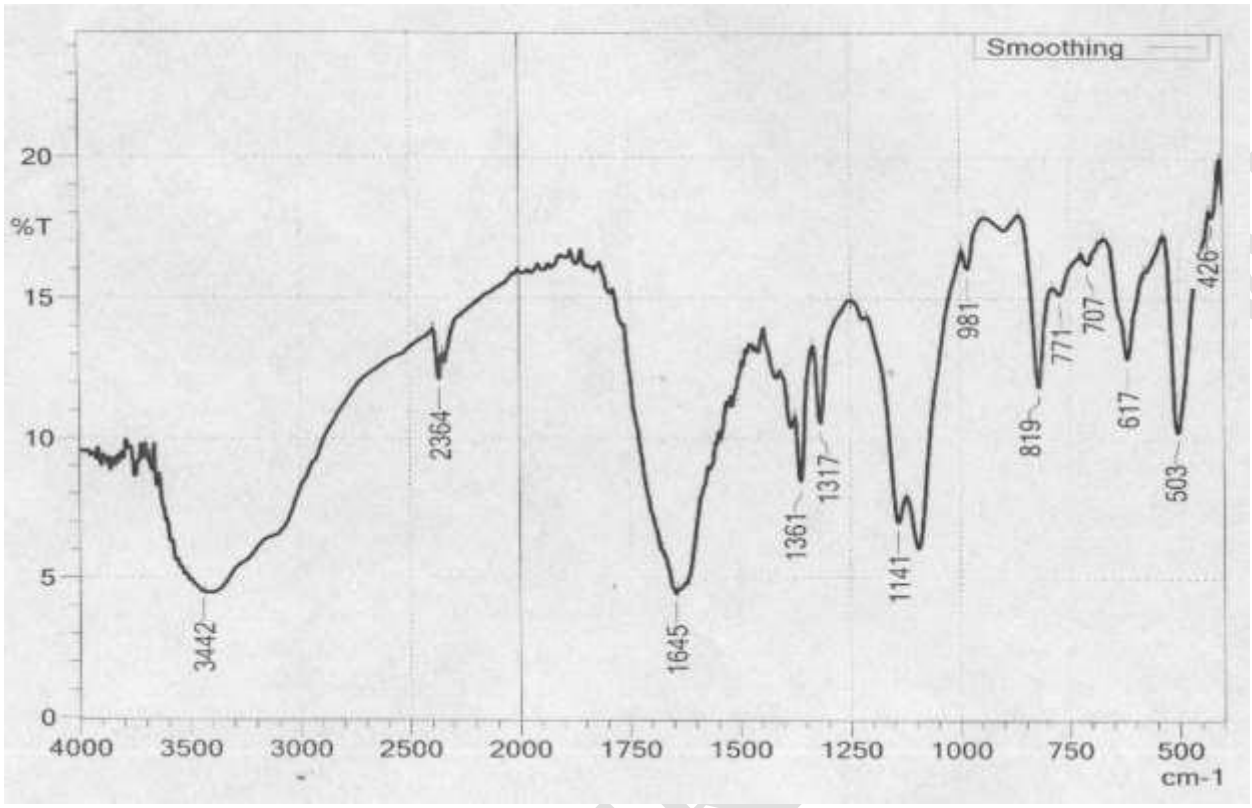

FT-IR spectrum of [Cu(Ita)(Thg)$(H_2O)_2$]

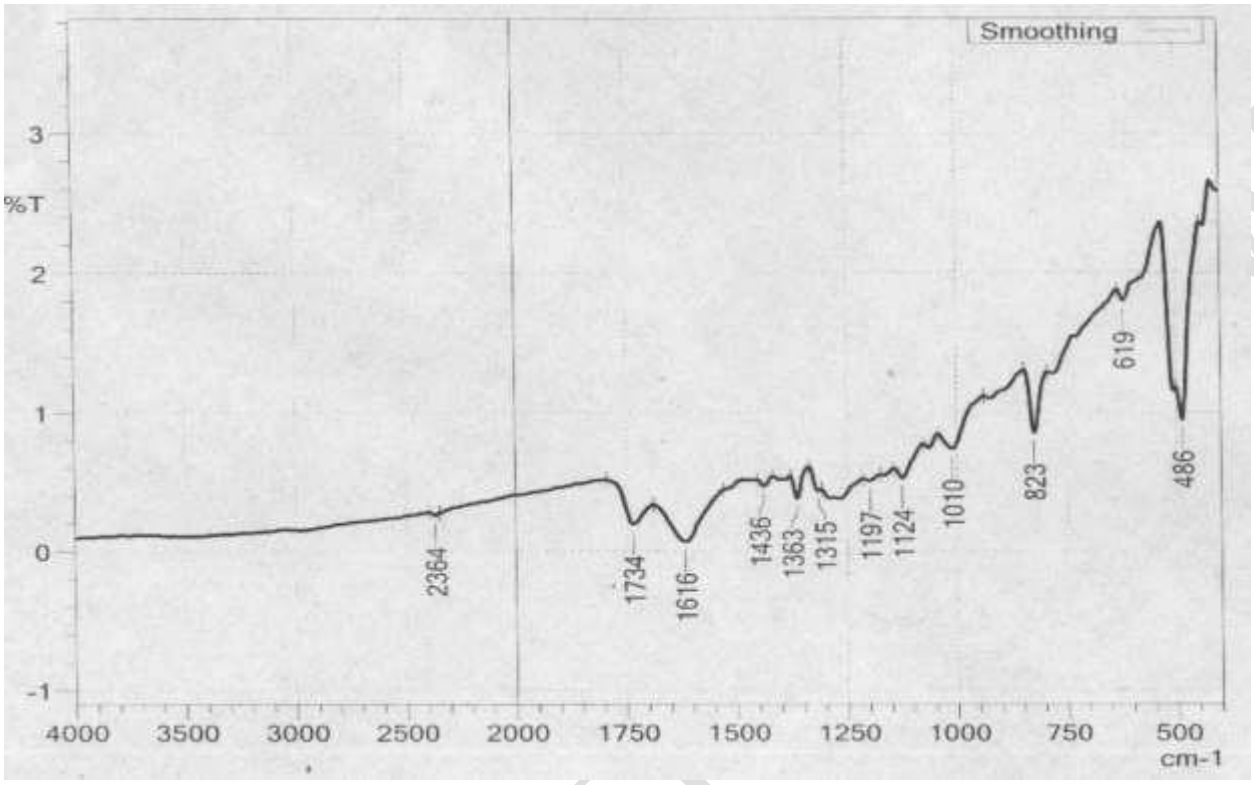

FT-IR spectrum of [Cu(Fum)(Thg)]

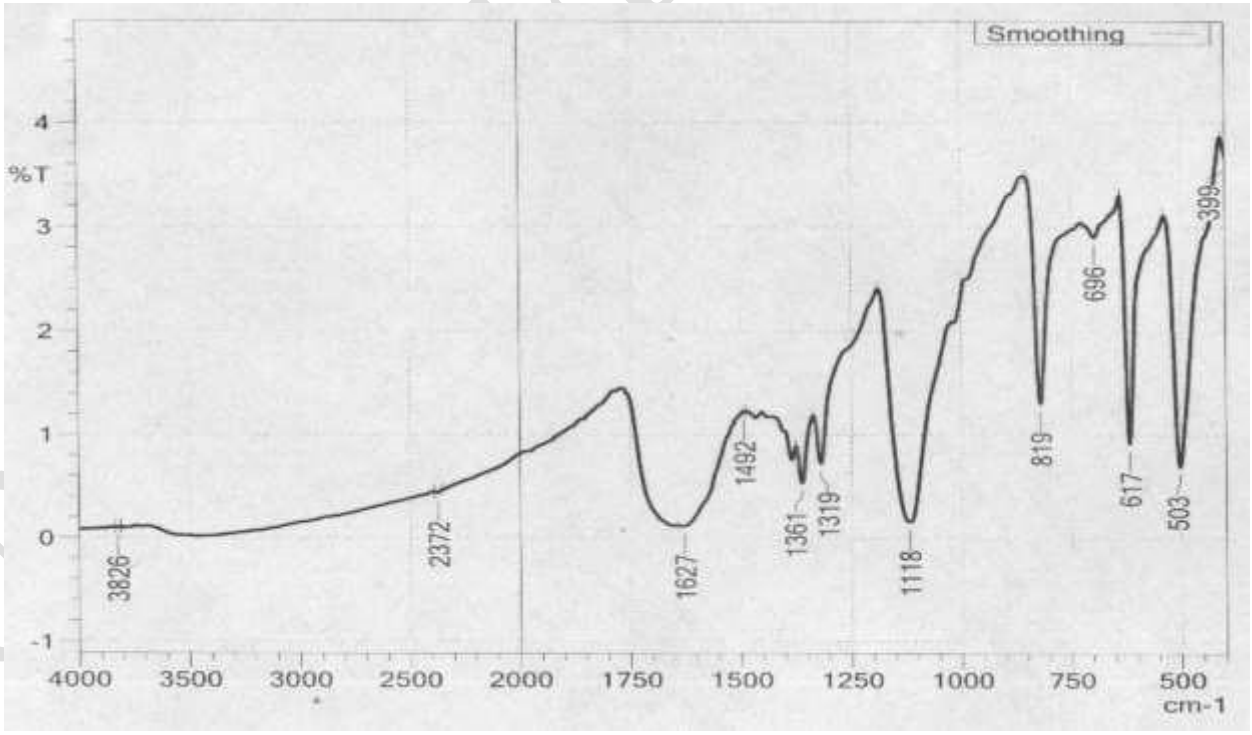

FT-

IR spectrum of [Cu(mal)(Thg)]

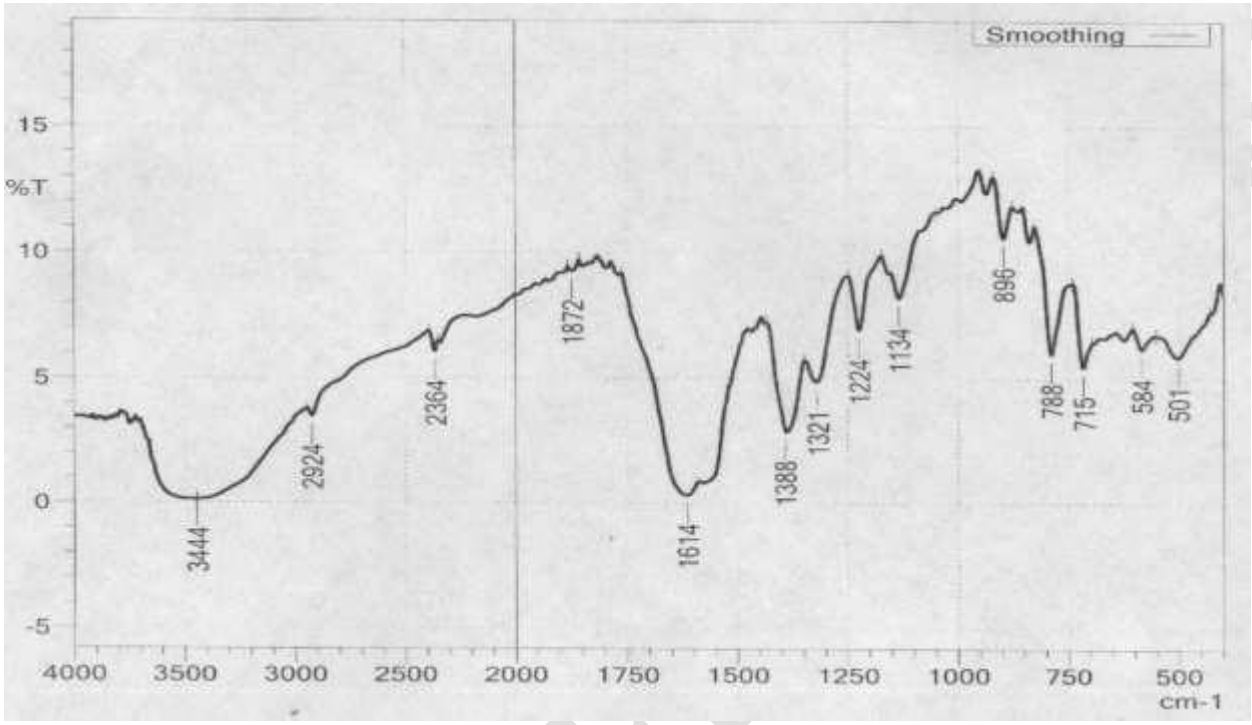

FT-IR spectrum of [Cd(Oxa)(Thg)(H_2O)$_2$]

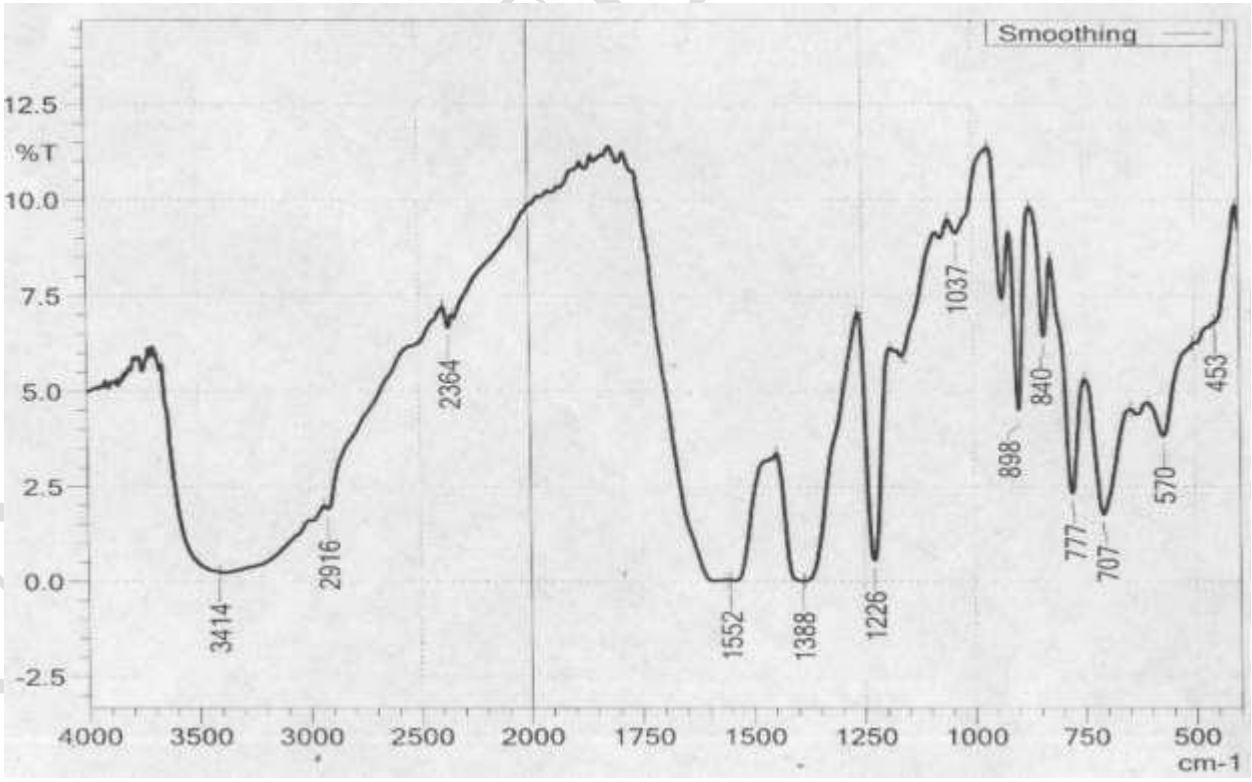

FT-

IR spectrum of [Cd(Ina)(Thg)(H_2O)$_2$]

3. FT-IR SPECTRA OF THIO-FUNCTIONALIZED MOFs.

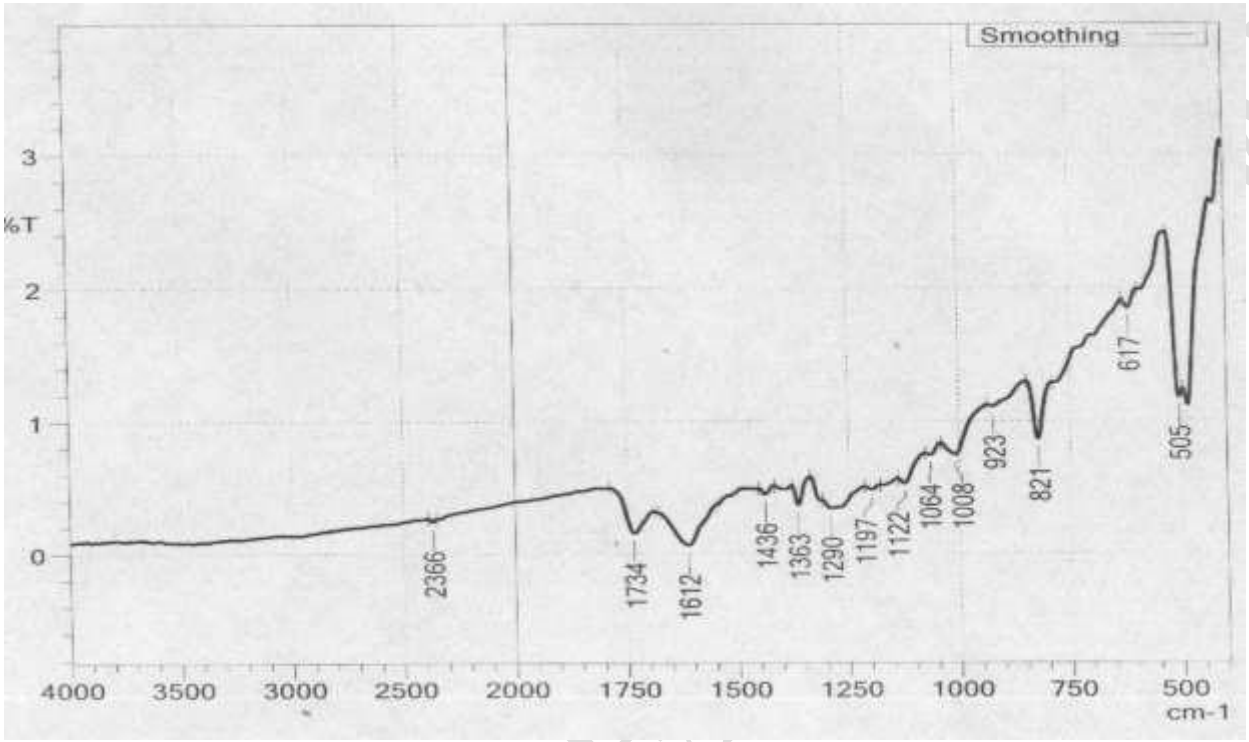

FT-IR spectrum of [Cu(INA)$_2$]-TH

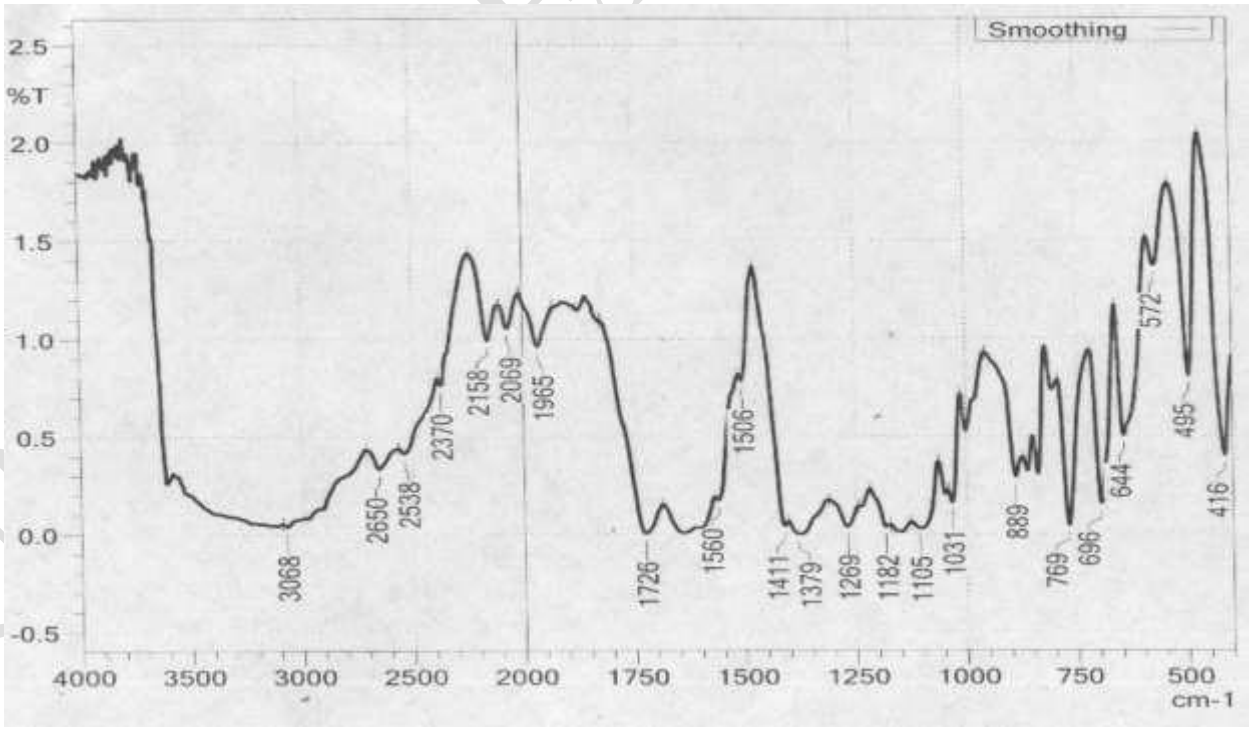

FT-

IR spectrum of $[Zn(INA)_2]$-TH

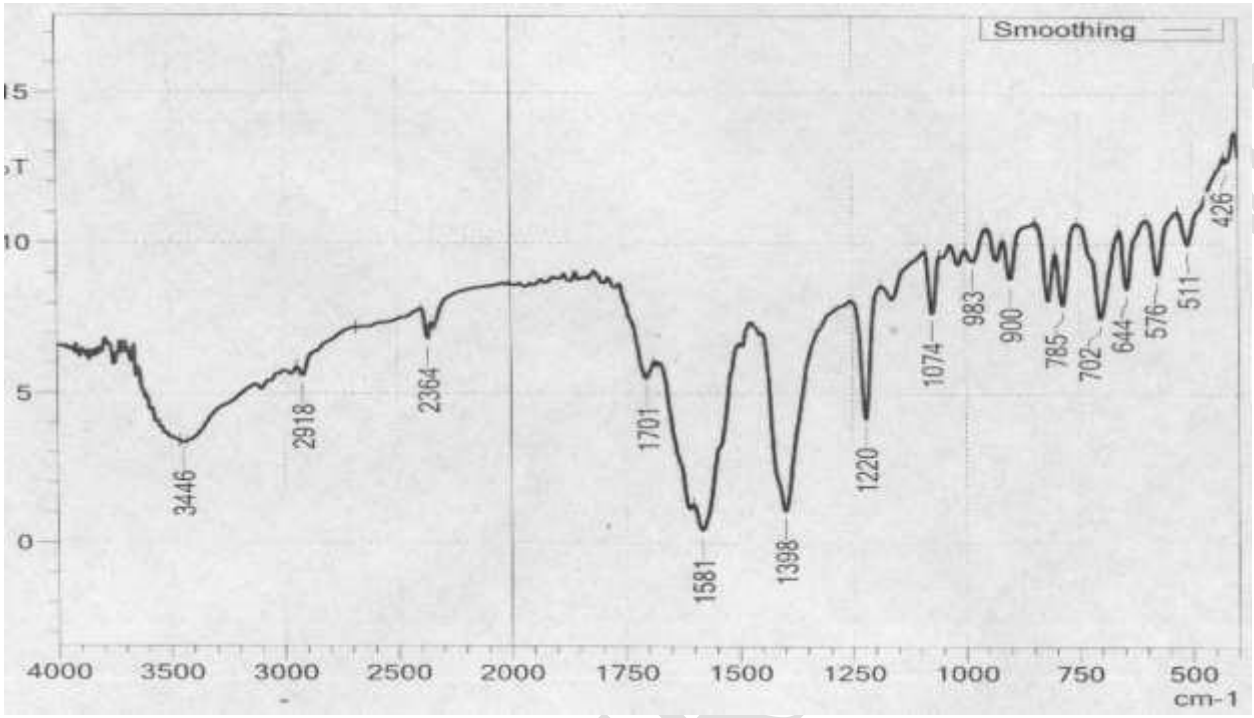

FT-IR spectrum of $[Zn(fum)_2(byp)]$-TH

FT-

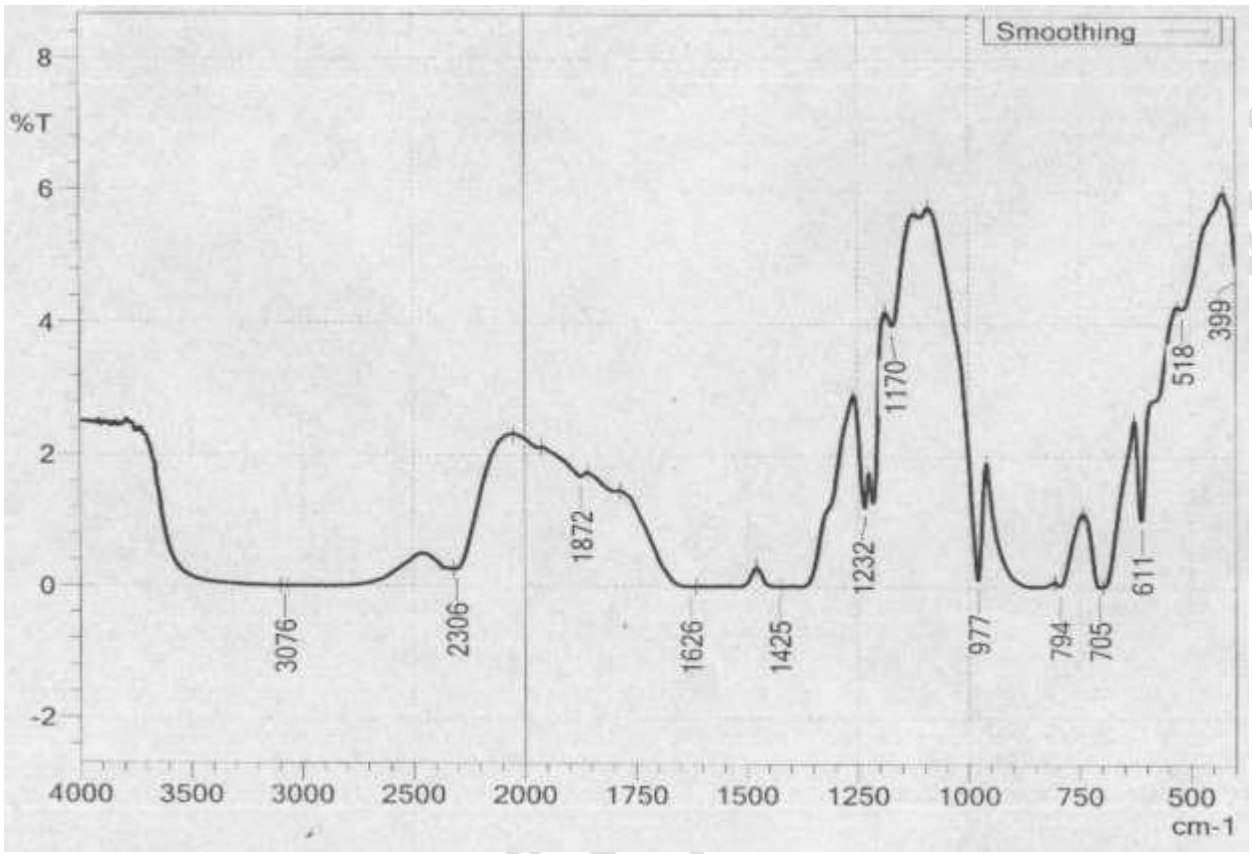

IR spectrum of [Zn(fum)(H_2O)$_2$]-TH

FT-